ISSN 1949-8470 (online)

World Journal of *Radiology*

World J Radiol 2023 July 28; 15(7): 216-240

Published by Baishideng Publishing Group Inc

World Journal of Radiology

Contents

Monthly Volume 15 Number 7 July 28, 2023

MINIREVIEWS

ORIGINAL ARTICLE

Basic Study

CASE REPORT

World Journal of Radiology

Monthly Volume 15 Number 7 July 28, 2023

Contents

ABOUT COVER

Editorial Board Member of *World Journal of Radiology*, Kıvanç Kamburoğlu, DDS, MSc, PhD, Professor, Department of Dentomaxillofacial Radiology, Ankara University, Ankara 06500, Turkey. dtkivo@yahoo.com

AIMS AND SCOPE

The primary aim of *World Journal of Radiology* (*WJR*, *World J Radiol*) is to provide scholars and readers from various fields of radiology with a platform to publish high-quality basic and clinical research articles and communicate their research findings online.

WJR mainly publishes articles reporting research results and findings obtained in the field of radiology and covering a wide range of topics including state of the art information on cardiopulmonary imaging, gastrointestinal imaging, genitourinary imaging, musculoskeletal imaging, neuroradiology/head and neck imaging, nuclear medicine and molecular imaging, pediatric imaging, vascular and interventional radiology, and women's imaging.

INDEXING/ABSTRACTING

The *WJR* is now abstracted and indexed in PubMed, PubMed Central, Emerging Sources Citation Index (Web of Science), Reference Citation Analysis, China National Knowledge Infrastructure, China Science and Technology Journal Database, and Superstar Journals Database. The 2023 Edition of Journal Citation Reports® cites the 2022 impact factor (IF) for *WJR* as 2.5; IF without journal self cites: 2.3; 5-year IF: 2.5; Journal Citation Indicator: 0.54.

RESPONSIBLE EDITORS FOR THIS ISSUE

Production Editor: *Si Zhao*; **Production Department Director:** *Xu Guo*; **Editorial Office Director:** *Jia-Ping Yan*.

NAME OF JOURNAL
World Journal of Radiology

ISSN
ISSN 1949-8470 (online)

LAUNCH DATE
January 31, 2009

FREQUENCY
Monthly

EDITORS-IN-CHIEF
Thomas J Vogl

EDITORIAL BOARD MEMBERS
https://www.wjgnet.com/1949-8470/editorialboard.htm

PUBLICATION DATE
July 28, 2023

INSTRUCTIONS TO AUTHORS
https://www.wjgnet.com/bpg/gerinfo/204

GUIDELINES FOR ETHICS DOCUMENTS
https://www.wjgnet.com/bpg/GerInfo/287

GUIDELINES FOR NON-NATIVE SPEAKERS OF ENGLISH
https://www.wjgnet.com/bpg/gerinfo/240

PUBLICATION ETHICS
https://www.wjgnet.com/bpg/GerInfo/288

PUBLICATION MISCONDUCT
https://www.wjgnet.com/bpg/gerinfo/208

ARTICLE PROCESSING CHARGE
https://www.wjgnet.com/bpg/gerinfo/242

STEPS FOR SUBMITTING MANUSCRIPTS
https://www.wjgnet.com/bpg/GerInfo/239

ONLINE SUBMISSION
https://www.f6publishing.com

World Journal of Radiology

Submit a Manuscript: https://www.f6publishing.com

World J Radiol 2023 July 28; 15(7): 216-225

DOI: 10.4329/wjr.v15.i7.216

ISSN 1949-8470 (online)

MINIREVIEWS

Progress of magnetic resonance imaging radiomics in preoperative lymph node diagnosis of esophageal cancer

Yan-Han Xu, Peng Lu, Ming-Cheng Gao, Rui Wang, Yang-Yang Li, Jian-Xiang Song

Specialty type: Radiology, nuclear medicine and medical imaging

Provenance and peer review: Unsolicited article; Externally peer reviewed.

Peer-review model: Single blind

Peer-review report's scientific quality classification

Grade A (Excellent): 0
Grade B (Very good): 0
Grade C (Good): C, C
Grade D (Fair): 0
Grade E (Poor): 0

P-Reviewer: Jeong KY, South Korea; Singh G

Received: April 18, 2023
Peer-review started: April 18, 2023
First decision: June 1, 2023
Revised: June 11, 2023
Accepted: June 30, 2023
Article in press: June 30, 2023
Published online: July 28, 2023

Yan-Han Xu, Ming-Cheng Gao, Rui Wang, Yang-Yang Li, Jian-Xiang Song, Department of Thoracic Surgery, Yancheng Third People's Hospital, Affiliated Hospital 6 of Nantong University, Yancheng 224000, Jiangsu Province, China

Peng Lu, Department of Imaging, Yancheng Third People's Hospital, Affiliated Hospital 6 of Nantong University, Yancheng 224000, Jiangsu Province, China

Corresponding author: Jian-Xiang Song, PhD, Chief Doctor, Department of Thoracic Surgery, Yancheng Third People's Hospital, Affiliated Hospital 6 of Nantong University, No. 500 Yonghe Road, Gangzha District, Yancheng 224000, Jiangsu Province, China.
jxsongycsy@163.com

Abstract

Esophageal cancer, also referred to as esophagus cancer, is a prevalent disease in the cardiothoracic field and is a leading cause of cancer-related mortality in China. Accurately determining the status of lymph nodes is crucial for developing treatment plans, defining the scope of intraoperative lymph node dissection, and ascertaining the prognosis of patients with esophageal cancer. Recent advances in diffusion-weighted imaging and dynamic contrast-enhanced magnetic resonance imaging (MRI) have improved the effectiveness of MRI for assessing lymph node involvement, making it a beneficial tool for guiding personalized treatment plans for patients with esophageal cancer in a clinical setting. Radiomics is a recently developed imaging technique that transforms radiological image data from regions of interest into high-dimensional feature data that can be analyzed. The features, such as shape, texture, and waveform, are associated with the cancer phenotype and tumor microenvironment. When these features correlate with the clinical disease outcomes, they form the basis for specific and reliable clinical evidence. This study aimed to review the potential clinical applications of MRI-based radiomics in studying the lymph nodes affected by esophageal cancer. The combination of MRI and radiomics is a powerful tool for diagnosing and treating esophageal cancer, enabling a more personalized and effectual approach.

Key Words: Esophageal cancer; Diffusion-weighted imaging; Dynamic contrast-enhanced imaging; Radiomics; Lymph nodes

Core Tip: Precise TNM staging is crucial for developing effective treatment plans for esophageal cancer. Establishing whether esophageal cancer has lymph node metastasis before surgery remains a significant clinical challenge. However, with the continuous advancement of radiomics, high-quality clinical decision support systems have emerged, enabling more accurate determination of preoperative lymph node status in esophageal cancer. This breakthrough may lead to formulating treatment plans that adhere to individualized medical guidelines.

Citation: Xu YH, Lu P, Gao MC, Wang R, Li YY, Song JX. Progress of magnetic resonance imaging radiomics in preoperative lymph node diagnosis of esophageal cancer. *World J Radiol* 2023; 15(7): 216-225
URL: https://www.wjgnet.com/1949-8470/full/v15/i7/216.htm
DOI: https://dx.doi.org/10.4329/wjr.v15.i7.216

INTRODUCTION

According to statistical studies, esophageal cancer is a prevalent malignant tumor of the digestive system, ranking seventh in incidence and sixth in mortality worldwide[1,2]. Endoscopic therapy, chemotherapy, and surgical resection are the primary treatments for esophageal cancer, with surgery being the leading treatment method for early-stage esophageal cancer[3]. Lymph node metastasis is an important prognostic factor in surgically treatable esophageal cancer[4-6]. While lymphatic spread in esophageal cancer is highly variable, positive lymph nodes should be resected along with the tumor to improve long-term survival[7,8]. However, extended lymph node resection may increase postoperative complications and worsen the prognosis of patients with esophageal cancer. Therefore, accurate lymph node evaluation is essential for developing an appropriate treatment strategy.

Magnetic resonance imaging (MRI) is more definitive than other imaging modalities in detecting positive lymph nodes in cancer and has been increasingly used in studying esophageal squamous cell carcinoma at the T and N stages[9-13]. Additionally, radiomics has gained momentum in cancer research over recent years[14]. Radiomics can quantify inter- and intratumor heterogeneity, accurately determine the status of preoperative lymph nodes in esophageal cancer and provide a better basis for clinical decisions regarding treatment options for esophageal cancer[15]. This paper reviews the research and applications of MRI, radiomics, and combined imaging techniques to determine the status of lymph nodes in esophageal cancer.

METASTATIC FEATURES OF ESOPHAGEAL CANCER LYMPH NODES AND THEIR IMPACT ON TREATMENT

Esophageal cancer commonly metastasizes to the lower neck, upper mediastinum, and perigastric area[16,17]. The lymph node metastasis rate (LNMR) primarily depends on the location and depth of tumor infiltration[18]. Therefore, certain lymph node regions, such as the cervical segmental paraoesophageal LN, the laryngeal recurrent nerve LN, and the LN along the left gastric artery, have a high LNMR[16].

Since the prognosis of patients with esophageal cancer mainly depends on the extent of the primary tumor and the lymphatic spread of the disease, lymph node status is a crucial prognostic factor[19,20]. Thus, clarifying the extent of lymph node dissection during surgical treatment is important for the prognosis of esophageal cancer. Tong and Kim *et al*. have demonstrated that patients with esophageal cancer with lymph node metastasis have a lower 5-year survival rate [19,21-23]. The lymph node ratio (absolute number of lymph nodes removed compared to the number of lymph nodes involved) in postoperative patients was an independent predictor of overall survival. Similar studies have indicated that residual lymph node metastasis after treatment is a critical indicator for assessing survival[24]. Therefore, an accurate assessment of the extent of lymph node metastasis in esophageal cancer provides an objective basis for clinical treatment planning and a reference value for patient regression after treatment.

The treatment options for esophageal cancer primarily depend on the TNM stage of the patient. According to Mönig *et al*[17] endoscopic resection is the recommended treatment for early superficial submucosal invasive carcinoma without histologic risk factors such as lymphatic or vascular infiltration. However, the rate of lymph node metastasis in submucosal carcinoma increases with the depth of infiltration. Therefore, the current gold standard of treatment for esophageal cancer is transthoracic subtotal esophagectomy and double field lymph node dissection[25].

The extent of lymph node dissection in esophageal cancer remains controversial[26]. A randomized study found no significant improvement in long-term survival with expanded transthoracic surgery in esophageal adenocarcinoma[27, 28]. Meanwhile, Lordick *et al*[29] concluded in their discussion of early management of esophageal cancer that surgery is considered standard of care for disease without suspected lymph node involvement (T1-2 N0 M0), and if lymph node involvement of disease is suspected (T1-2 N1-3 M0), patients are recommended to undergo preoperative treatment. Only after evaluation without involvement of lymph nodes should surgery be considered. Therefore, accurately diagnosing preoperative lymph nodes remains a challenge to be addressed.

RESEARCH PROGRESS OF MRI IN LYMPH NODES OF ESOPHAGEAL CANCER

After the diagnosis of esophageal cancer is confirmed by endoscopy and biopsy, staging is crucial for treatment and prognosis. Traditional examination methods, including endoscopic ultrasound (EUS) and computed tomography (CT), play an important role in determining T stage, invasiveness of surrounding structures, and detecting distant metastases [30,31]. Recent studies have shown that 18F-fluoro-2-deoxyglucose positron emission tomography (FDG-PET/CT) examination is also valuable in detecting distant metastases[32]. However, EUS, CT, and FDG-PET(/CT) have limitations in detecting lymph node involvement, which is an important independent predictor of long-term survival in patients[33].

CT scans are commonly used as a non-invasive method to assess metastatic infiltration of esophageal cancer lymph nodes. In CT diagnosis, intra-thoracic lymph nodes with a short diameter greater than 10 mm are considered metastatic lymph nodes. However, some studies have shown that only a small percentage of metastatic lymph nodes in esophageal cancer have a short diameter greater than 10 mm[33,34].

Furthermore, a related study found that although the sensitivity of CT was 59% in detecting lymph nodes larger than 10 mm in the conventional lymph node region of esophageal cancer, the diagnostic value of lymph nodes with metastasis was still insufficient[35]. Measuring the long and short axis diameters of lymph nodes in each region of esophageal cancer in CT images and calculating the axis ratio could improve the sensitivity of CT detection of lymph node metastasis in esophageal cancer. However, the sensitivity, specificity, and accuracy of this approach are still insufficient to provide high-quality clinical decision support systems[36].

MRI is superior to CT in terms of soft tissue resolution and can accurately detect differences in water content in tissues. Its images are unique in their ability to discriminate between masses, lymph nodes, and vascular structures from each other. MRI has multi-sequence imaging and multiple image types, and can generate images from multiple levels (cross-sectional, sagittal, coronal, and various oblique views) at will, reducing the artifacts of soft tissue boundaries in the images and providing richer imaging information to clarify the nature of the lesion. Although MR imaging modalities primarily focus on morphologic changes and provide less functional information about the tumor and are not the preferred method for staging, recent studies have shown that with the technical development of diffusion-weighted imaging (DWI), dynamic contrast-enhanced (DCE)-MRI, and IVIM, MR is progressively more accurate than CT in determining resectability, mediastinal invasion, and especially lymph node involvement[37].

DWI can provide information on tissue structure and cell density by reflecting the measured apparent diffusion coefficient (ADC) of water molecule mobility, and this quantitative metric is considered a meaningful imaging biomarker in esophageal studies[38]. Since its introduction into clinical practice, DWI has been widely used to detect lymph node metastasis in various primary malignancies and is a successful method[39]. In a prognostic study of esophageal cancer treatment, Giganti *et al*[38] found that pathological ADC could be considered a prognostic factor in esophageal cancer, and DWI may become a promising and reliable diagnostic technique for esophageal cancer. Sakurada *et al*. also found that the DWI-MRI imaging technique is important in determining the lymph node status of patients with esophageal cancer by visualizing lymph nodes and performing ADC value measurement[40]. In a quantitative analysis study by Alper *et al*[34] it was found that the STIR sequence improved the detection of metastatic lymph nodes with a sensitivity of 81.3% and a specificity of 98.3%, which is consistent with the findings of the group. While the diagnostic performance of DWI and PET for lymph nodes is controversial, the study by Shuto *et al*[39] concluded that DWI showed a higher sensitivity than PET in terms of diagnostic performance of lymph nodes. Given the association between lymph node status and prognosis in esophageal cancer, we believe that DWI is a predictive modality for survival after surgery in patients with esophageal cancer.

DCE-MRI has proven useful as a functional MRI modality in assessing vascular perfusion for monitoring and predicting response to radiotherapy. The histogram analysis established in DCE-MRI is a means of extracting heterogeneous parameters from significant regions (ROI) and whole-tumor analysis of samples from the entire tumor parenchyma and interstitium that can provide a more accurate quantitative assessment of tumor biology[41]. This technique has improved the diagnostic capability of MRI. In the study by Sun *et al*[42] on radiotherapy for esophageal cancer, the results of different histogram parameters (median, mean, standard deviation, mode, skewness, kurtosis, minimum, maximum, percentile, and entropy) derived from DCE-MRI were compared and found to be useful for the assessment of tumor heterogeneity and monitoring the response to radiotherapy for esophageal cancer. Regarding lymph node status analysis, the findings of Chen *et al*[41] suggest that whole-tumor cumulative histogram analysis obtained from DCE-MRI with pharmacokinetics as a parameter may be useful for T-staging and regional lymph node status determination in esophageal squamous cell carcinoma. Although the study of lymph node status in esophageal cancer by DCE-MRI is still in its infancy, the available data and results show that DCE-MRI has a high accuracy in determining lymph node status, which is important for developing individualized treatment plans for esophageal cancer.

Recently, the StarVIBE sequence on MRI has been utilized in cases where patients are unable to hold their breath and has gradually been incorporated into studies on esophageal cancer[12,43]. Qu *et al*[44] conducted a study where MRI was shown to better predict lymph node status in patients with preoperative esophageal cancer by extracting the ROI of esophageal cancer lesions. This method demonstrated significantly improved diagnostic accuracy over CT and could facilitate better treatment planning for esophageal cancer. Therefore, MRI shows promise in aiding lymph node assessment in esophageal cancer patients, particularly when CT scans yield inconclusive results. Nevertheless, further research is required to confirm its effectiveness in clinical practice.

While the clinical value of MRI in lymph node diagnosis, treatment evaluation, and prognosis prediction has been gradually recognized, false-positive lymph nodes can also occur on MRI due to interference from cardiac motion and gastric peristaltic artifacts. Moreover, false-negative lymph nodes can also be observed in smokers and patients with pneumoconiosis or silicosis with esophageal cancer[45]. Despite advancements in radiological examination methods, further improvement in the sensitivity of lymph node metastasis determination may still be possible. For instance, the

development of new imaging techniques or the integration of multiple imaging modalities could potentially improve the accuracy of lymph node metastasis detection in esophageal cancer patients. Additionally, further studies focusing on the optimization of imaging protocols and the standardization of image interpretation criteria may lead to more accurate and reliable diagnosis of lymph node metastasis.

Process steps of radiomics

Radiomics is the application of computerized mathematical tools to image processing, transforming image data from ROI in radiological images into mineable high-dimensional feature data. The radiological features (*e.g.*, shape, texture, or waveform) extracted from them can provide information about the cancer phenotype as well as the tumor microenvironment[14]. This information is distinct and complementary to other disease-related information, including clinical features, treatment-related decision information, or genomic data[46]. When radiomics-derived data are combined with other relevant data and correlated or extrapolated to clinical disease outcomes, they can produce accurate and reliable clinical decision support systems (CDSS). These CDSS can assist clinicians in making more informed decisions regarding diagnosis, treatment planning, and prognosis prediction for patients with esophageal cancer (Figure 1).

Radiomics refers to the quantitative mapping of medical images, involving the extraction and analysis of numerous image features that are relevant to the study objectives, including clinical treatment decisions and genomic features. Radiomics studies typically encompass five phases, namely data selection, medical imaging, feature extraction, exploratory analysis, and modeling. The analysis of radiomics can be localized in the primary tumor foci, metastatic lesions, or normal tissues or can be applied to any image generated in the clinical setting. Radiomics analysis can provide valuable insights into tumor heterogeneity and microenvironment, which can aid in identifying potential biomarkers for prognosis and treatment response prediction in patients with esophageal cancer. However, further research is necessary to validate the clinical utility of radiomics in esophageal cancer and to establish standardized protocols for radiomics analysis.

Regarding image feature extraction in radiomics, it involves extracting quantitative features from images that represent the volume of interest (VOI), which are eigenvalues of an image that depend on factors such as image preprocessing (*e.g.*, filtering or intensity discretization) and reconstruction (*e.g.*, filtered backprojection or iterative reconstruction)[14]. Delineating the ROI or VOI is a critical first step in any radiomics method. However, manual, and semi-automatic segmentation methods often introduce observer bias and can be time-consuming. Additionally, inter-, and intra-observer variation in ROI/VOI delineation can affect the reproducibility and stability of radiomics features. Therefore, studies using manual or semi-automatic segmentation with manual correction should evaluate the internal and external reproducibility of derived radiomics features. To ensure result reproducibility, it is advisable to exclude irreproducible features from further analysis. Automating the segmentation process using deep learning techniques has also shown promise in improving the reproducibility and efficiency of ROI/VOI delineation in radiomics studies.

The second step in image processing is a crucial intermediary between image segmentation and feature extraction. Its objective is to standardize the images for radiomics feature extraction, including pixel spacing, grayscale intensities, and gray histogram binning, among other factors. The reliability of test-retest of extracted radiomics features depends on the image processing settings used in this step. Therefore, it is critical to carefully select and optimize the image processing settings to ensure the robustness and reproducibility of radiomics features. The pyRadiomics package, which is one of the most widely used packages for radiomics analysis, allows various image processing steps to be defined through a parameter file in YAML or JSON structured text format. This file can then be loaded into 3D Slicer or integrated into a Python framework to facilitate feature calculation.

After image segmentation and processing, the third step of radiomics feature extraction can be performed. Feature extraction involves calculating feature descriptors to quantify the gray-level features within the ROI/VOI. As there are many ways and formulas to calculate these features, it is recommended to follow the Image Biomarker Standardization Initiative (IBSI) guidelines[47].

The IBSI guidelines provide a consensus for standardized feature calculations from a matrix of all radiomics features. Different types of radiomics features exist, including intensity-based (histogram) features, shape features, texture features, transform-based features, and radial features, with different types of filters (*e.g.*, wavelet or Gaussian filters) usually applied in the feature extraction step. After feature selection/deviation is performed, subsequent statistical analysis and machine learning will be used to identify the important features that support image analysis. Dimensionality reduction is a multi-step process to exclude irreducible, redundant, and irrelevant features from the dataset.

The first step involves excluding non-replicated features, as a feature that has high intra- or inter-observer variability may be less likely to be useful. The second step is to select the most relevant variables for the corresponding task. Various methods that often rely on machine learning techniques can be used for this initial feature selection step, such as elimination filters, recursive feature elimination methods, or random forest algorithms. As these algorithms often cannot account for covariance and correlation in the data, constructing correlation clusters is the logical next step in the dimensionality reduction workflow. In some cases, this step may be combined with the previous (second) step, as few machine learning techniques can handle correlations in the data. Correlation clustering allows the visualization of highly correlated features in the data and the selection of only one representative feature per correlation cluster.

Selecting the variable with the highest bio-clinical variability in the dataset is crucial as it is likely to be the most representative of the variation within a given patient population. Once the dimensionality of the data has been reduced, the importance of the data visualization step increases. Therefore, reducing the number of features used to build statistical and machine learning models through a step called feature selection or dimensionality reduction is critical to generating valid and generalizable results. The remaining uncorrelated and highly correlated features can be used to train models for the corresponding classification tasks, and the constructed radiomics models are evaluated according to the radiomics quality score. These key steps form the basis for ensuring that the imaging histology produces high-quality CDSS.

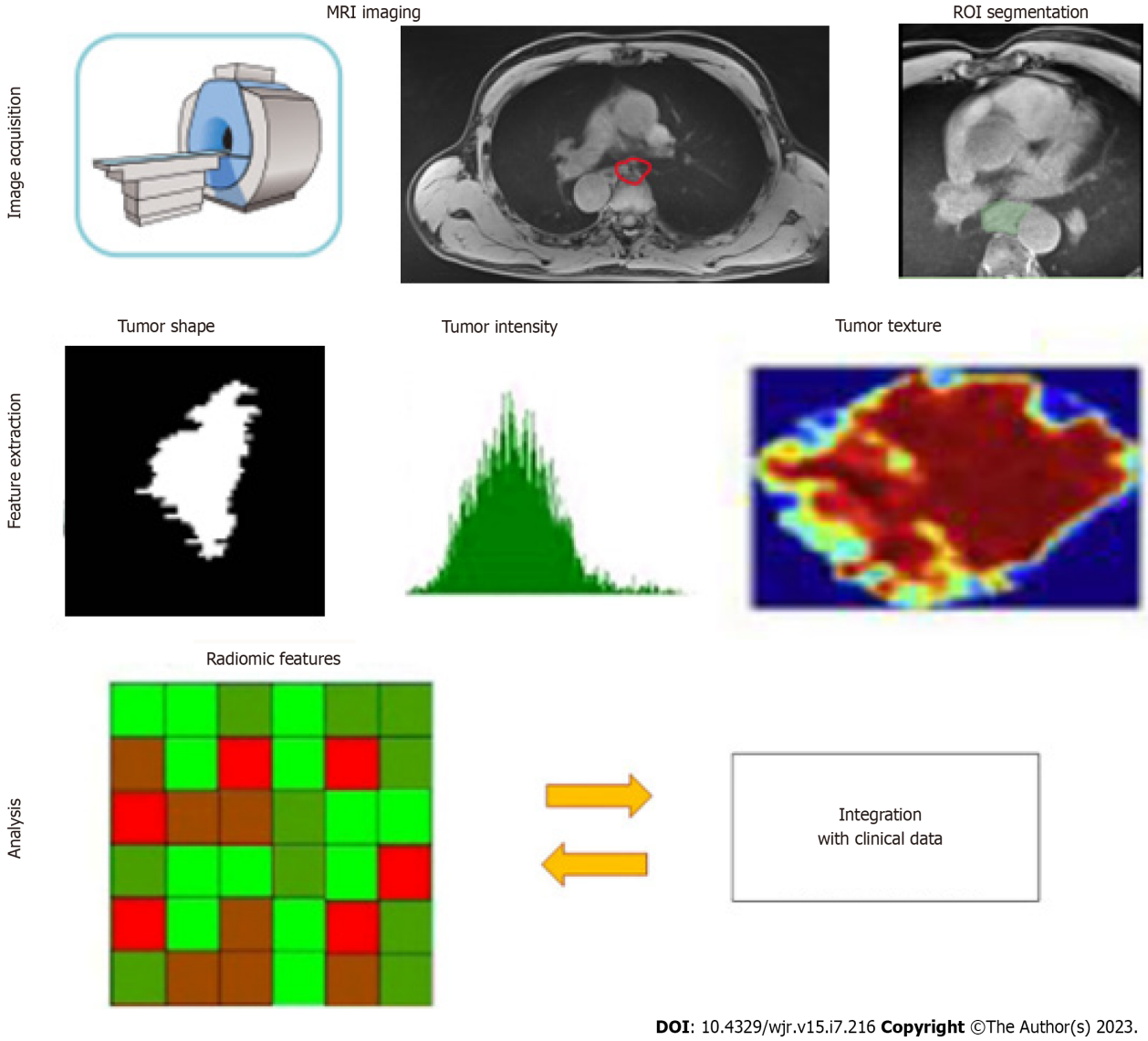

DOI: 10.4329/wjr.v15.i7.216

Figure 1 Research flow chart of radiomics based on magnetic resonance imaging in esophageal cancer. MRI: magnetic resonance imaging; ROI: Regions of interest.

Progress of CT radiomics in esophageal cancer lymph nodes

When radiomics is involved in tumor exploration, it provides a new approach in the study of cancer patients by developing and validating an imaging-based radiomic columnar map that combines radiomic features and clinical factors in the development of cancer patients. In the esophageal cancer study discussed in this article, there have been many researchers, in recent years, who have applied radiomics to the study of esophageal cancer, thus showing that radiomics is not a novel technique.

Li *et al*[48] extracted radiomic features from FDG-PET images of 152 patients with esophageal cancer and successfully predicted those patients who would not benefit from preoperative radiotherapy. Qiu *et al*[49] developed and validated a CT-based radiomic columnar map that combined radiomic features and clinical factors to predict the risk of recurrence in patients who underwent surgery after neoadjuvant chemotherapy and achieved a pathologic complete response in patients with esophageal cancer at risk of recurrence. Meanwhile, in terms of lymph nodes, which are the focus of this article, Gu *et al*[50] studied 129 sets of lymph nodes from 77 patients in the cohort (trial cohort: 102 lymph nodes from 59 patients; validation cohort: 27 lymph nodes from 18 patients) based on the radiomic features of CT to predict the treatment response and the ability of local control of locally recurrent lymph nodes after radiotherapy esophagectomy. A scoring model based on the location and length of the cancer focus and the size and status of the corresponding lymph node region as revealed by CT allowed for accurate assessment of the status of the lymph nodes, which helped in the development of the surgical approach and accurate intraoperative clearance of the corresponding lymph nodes. Meanwhile, in a case-control study of esophageal cancer, Qu *et al*[44] extracted radiomic features from CT data of 152 patients with esophageal cancer without lymph node metastases and 182 patients with lymph node metastases and found that CT radiologic features could help predict the lymph node status of patients with advanced esophageal cancer and effectively distinguish whether there were regional lymph node metastases in esophageal cancer. Moreover, Tan *et al*[51] retrospectively analyzed 230 patients with esophageal cancer who had CT examinations and found that radiomics could

help reveal intra-tumor heterogeneity and could be used as a new biomarker to determine LN status in patients with resectable esophageal cancer by using a radiomic column line graph containing 5 features in combination with CT-reported LN status (*i.e.*, size criteria). This shows that the CT radiomics model can be applied clinically to assess the lymph node status in patients with esophageal cancer prior to treatment.

Although most current radiomic studies of ESCC are based on CT and PET, preoperative MRI radiologic features are more valuable because MRI is noninvasive and has higher tissue resolution. Qu *et al*[44] 50 of 181 patients with pathologically confirmed esophageal cancer with lymph node metastases, based on T2-TSE-BLADE and StarVIBE enhancement sequences in MRI images. Nine radiographic features were selected to create radiographic features significantly associated with LN metastasis, and the model was found to distinguish well between metastatic and non-metastatic lymph nodes.

Development of MRI radiomics in tumor research

Although most of the current radiomic studies of ESCC are based on CT and PET, with the advancement of MRI techniques such as DWI, DCE-MRI, and IVIM, and the availability of high-quality imaging sequences such as the related StarVIBE and T2_BLADE, MRI has excellent soft-tissue resolution and is more conducive to the mutual discrimination between lesions, lymph nodes, and vascular structures. MRI findings such as the size, morphology, and shape of cancer foci are important for their identification in the study of tumor subtypes[52,53]. In some studies, it has been found that some specific MRI sequences can better detect lesions and aid in treatment selection[53]. The ROI generated from MRI images can be analyzed by imaging histology to extract superior imaging features. These features can be combined with clinically relevant patient information to generate high-quality CDSS to guide treatment planning.

ROI analysis of the primary tumor lesion not only yields key information about the relevant pathology but also has value for the prognostic analysis of patient survival. Shin *et al*[54] applied an MRI radiomic model to assess the pathological remission response in rectal cancer patients receiving neoadjuvant radiotherapy and found that the diagnostic value was superior to visual assessment by an experienced radiologist. Meanwhile, Li *et al*[48] extracted radiomic features from T2-weighted MRI images and combined them with clinical data for deep machine learning, which stably predicted the survival of glioma patients and helped to preoperatively assess the extent of macrophage infiltration in glioma tumors[55].

Although there is increasing interest in MRI radiomics in various areas of oncology across studies, most of the studies have focused almost exclusively on the histological and radiomic features associated with the primary tumor. It is well-known that histopathological data of the primary tumor, such as lymph-vascular invasion, histological grading, and tumor markers, are important factors used to guide or determine clinical treatment decisions. Meanwhile, when MRI radiomics is focused on the diagnosis of preoperative lymph node status, its high-quality diagnostic results can further guide treatment decisions in the clinical setting. In a study by Santucci *et al*[56], they found 3T MRI radiomics combined with histological data could predict preoperative lymph node metastasis in breast cancer patients and guide treatment planning. The results suggest that accurate prediction of lymph node status can avoid invasive surgery, such as lymph node dissection or biopsy[56]. Similar conclusions were reached in studies on the prediction of preoperative lymph node status in breast cancer, suggesting that the influential features of MRI radiomics are important for the determination of lymph node status[57-59].

It is worth noting that while the image features derived solely from the ROI of cancer foci can be used to analyze the status of lymph nodes, the CDSS obtained from both the ROI of lymph nodes and cancer foci is more clinically valuable when combined for imaging histological analysis. In Li *et al*.'s study, they combined the ROIs of both primary colon cancer lesions and lymph node lesions for imaging histological analysis, and their findings were even more convincing because they required the analysis of both cancer lesion features and lymph node features in their derived nomogram features[60].

While various high-quality MRI sequences have been studied, the analysis of optimal imaging sequences is still rare. Qu *et al*[44] selected 9 radiographic features based on the T2-TSE-BLADE and Star-VIBE enhancement sequences in MRI images to create radiographic features that are significantly associated with LN metastasis in 181 patients with pathologically confirmed lymph node metastasis. They found that the model based on this sequence effectively distinguished between metastatic and non-metastatic lymph nodes[44].

It is important to note that MRI examinations typically have a long examination time, and tumors that originate in the chest may be affected by the patient's respiratory movements, making artifacts unavoidable. While imaging histology can help reduce the impact of artifacts, it may also be beneficial to minimize examination time and extract established imaging histological features from optimal sequences to improve CDSS quality.

In oncology patients, accurately diagnosing lymph node status is critical for determining appropriate treatment options. While existing MRI radiomics studies have demonstrated its effectiveness in determining lymph node status, studies targeting focal radiomic features that link tumor features with lymph node status remain relatively uncommon. Analyzing various MRI sequences to identify sequences that yield high-quality imaging histological features may be an important area for future research.

Radiomics has garnered significant attention from researchers worldwide for its non-invasive, quantitative, and low-cost approach in diagnosing tissue characteristics, tumor staging, and treatment response. The current focus of radiomics research for esophageal cancer is on evaluating patient response and survival prognosis after different treatments. While predicting preoperative lymph node status using radiomics remains relatively rare, the numerous studies exploring various aspects of radiomics in esophageal cancer offer optimism for future research into using radiomics more widely to evaluate lymph nodes.

CONCLUSION

Although MRI has shown a trend toward superiority over other imaging methods for determining the lymph node status of esophageal cancer, the interference of respiratory motion and heartbeat specific to the chest and the presence of artifacts in imaging can affect the diagnosis of the lymph node status of esophageal cancer. Radiomics techniques use a combined medical-mathematical tool approach to convert conventional images into digital quantitative features, which have the potential to tap into the underlying biological features and heterogeneity of tumor images and have been widely used for diagnosis, differential diagnosis, and disease assessment. Radiomics can significantly improve the diagnostic specificity of lymph nodes.

However, MRI-based radiomics has not been extensively studied in esophageal cancer lymph nodes. Although some studies have found that MRI-based radiomic features are associated with lymph node metastasis, most were relatively small-sample and single-center studies, and the applicability and generalizability of the findings require further validation. The specificity of various MRI sequences and techniques for diagnosing lymph node status in esophageal cancer needs to be compared, and the quality of the images formed by the selected MRI sequences needs to be validated against histological data. Furthermore, a multicenter study should be conducted to increase the sample size and validate our findings. Successful completion of these essential steps can lead to the development of a valuable clinical decision support systems (CDSS) for esophageal cancer.

It is important to note that while radiomics analysis can be performed on medical images from different modalities, integrating cross-modality approaches using the potential information extracted from MRI, computed tomography, and PET can provide added value compared to evaluating each modality separately. However, the level of research sophistication still has low stability and generalizability, and specific study conditions and author selection can strongly influence the results.

In addition, most radiomic studies are based on retrospective data, resulting in a low evidence level. Therefore, prospective studies for validation in external cohorts or confirmatory studies, besides larger patient cohorts, are necessary to provide more reliable and generalizable results. Future studies should focus on developing standardized radiomics protocols and establishing open-access radiomics databases to promote the reproducibility and transparency of radiomics research. Radiomics has great overall potential for aiding clinical decision-making and improving patient outcomes; however, further validation and standardization are needed to ensure clinical utility.

It is essential to ensure that the imaging histology study is of high quality, addresses actual clinical needs, and can be implemented clinically to increase the likelihood of clinically relevant and valuable radiomics studies. Obtaining all relevant non-imaging data, such as demographics and bioinformatics, is critical. Standardizing the acquired images before performing radiomics analysis is essential to minimize the impact of different settings on the modeling. Implementing these key steps can lead to the formation of a valuable CDSS.

Furthermore, we believe that combining various MRI techniques and radiomics studies on esophageal cancer lymph nodes can introduce new quantitative imaging markers for medical imaging. With the precise determination of lymph node status using different MRI techniques and high-quality CDSS provided by radiomics findings, this approach may lead to significant breakthroughs in clinical studies. Preoperative personalized clinical characterization and precise treatment planning for esophageal cancer are possible with the introduction of new quantitative imaging markers.

FOOTNOTES

Author contributions: Xu YH contributed mainly to this work; Xu YH, Lu P, Gao MC, Wang R, Li YY, Song JX designed research; Xu YH, Lu P and Gao MC performed research; and Xu YH wrote the paper.

Conflict-of-interest statement: The author(s) declared no potential conflicts of interest with respect to the research, authorship, and/or publication of this article.

Country/Territory of origin: China

ORCID number: Yan-Han Xu 0000-0001-6230-4729; Jian-Xiang Song 0000-0003-4503-6464.

S-Editor: Ma YJ
L-Editor: A
P-Editor: Zhao S

REFERENCES

1 **Bray F**, Ferlay J, Soerjomataram I, Siegel RL, Torre LA, Jemal A. Global cancer statistics 2018: GLOBOCAN estimates of incidence and

mortality worldwide for 36 cancers in 185 countries. *CA Cancer J Clin* 2018; **68**: 394-424 [PMID: 30207593 DOI: 10.3322/caac.21492]

2 **Chen W**, Zheng R, Baade PD, Zhang S, Zeng H, Bray F, Jemal A, Yu XQ, He J. Cancer statistics in China, 2015. *CA Cancer J Clin* 2016; **66**: 115-132 [PMID: 26808342 DOI: 10.3322/caac.21338]

3 **Ishihara R**. Endoscopic Diagnosis and Treatment of Superficial Esophageal Squamous Cell Cancer: Present Status and Future Perspectives. *Curr Oncol* 2022; **29**: 534-543 [PMID: 35200548 DOI: 10.3390/curroncol29020048]

4 **Hofstetter W**, Correa AM, Bekele N, Ajani JA, Phan A, Komaki RR, Liao Z, Maru D, Wu TT, Mehran RJ, Rice DC, Roth JA, Vaporciyan AA, Walsh GL, Francis A, Blackmon S, Swisher SG. Proposed modification of nodal status in AJCC esophageal cancer staging system. *Ann Thorac Surg* 2007; **84**: 365-73; discussion 374 [PMID: 17643602 DOI: 10.1016/j.athoracsur.2007.01.067]

5 **Mariette C**, Piessen G, Briez N, Triboulet JP. The number of metastatic lymph nodes and the ratio between metastatic and examined lymph nodes are independent prognostic factors in esophageal cancer regardless of neoadjuvant chemoradiation or lymphadenectomy extent. *Ann Surg* 2008; **247**: 365-371 [PMID: 18216546 DOI: 10.1097/SLA.0b013e31815aaadf]

6 **Rice TW**, Lerut TE, Orringer MB, Chen LQ, Hofstetter WL, Smithers BM, Rusch VW, van Lanschot J, Chen KN, Davies AR, D'Journo XB, Kesler KA, Luketich JD, Ferguson MK, Räsänen JV, van Hillegersberg R, Fang W, Durand L, Allum WH, Cecconello I, Cerfolio RJ, Pera M, Griffin SM, Burger R, Liu JF, Allen MS, Law S, Watson TJ, Darling GE, Scott WJ, Duranceau A, Denlinger CE, Schipper PH, Ishwaran H, Apperson-Hansen C, DiPaola LM, Semple ME, Blackstone EH. Worldwide Esophageal Cancer Collaboration: neoadjuvant pathologic staging data. *Dis Esophagus* 2016; **29**: 715-723 [PMID: 27731548 DOI: 10.1111/dote.12513]

7 **Hosch SB**, Stoecklein NH, Pichlmeier U, Rehders A, Scheunemann P, Niendorf A, Knoefel WT, Izbicki JR. Esophageal cancer: the mode of lymphatic tumor cell spread and its prognostic significance. *J Clin Oncol* 2001; **19**: 1970-1975 [PMID: 11283129 DOI: 10.1200/JCO.2001.19.7.1970]

8 **Visser E**, van Rossum PSN, Ruurda JP, van Hillegersberg R. Impact of Lymph Node Yield on Overall Survival in Patients Treated With Neoadjuvant Chemoradiotherapy Followed by Esophagectomy for Cancer: A Population-based Cohort Study in the Netherlands. *Ann Surg* 2017; **266**: 863-869 [PMID: 28742691 DOI: 10.1097/SLA.0000000000002389]

9 **Dappa E**, Elger T, Hasenburg A, Düber C, Battista MJ, Hötker AM. The value of advanced MRI techniques in the assessment of cervical cancer: a review. *Insights Imaging* 2017; **8**: 471-481 [PMID: 28828723 DOI: 10.1007/s13244-017-0567-0]

10 **Moreno CC**, Sullivan PS, Mittal PK. MRI Evaluation of Rectal Cancer: Staging and Restaging. *Curr Probl Diagn Radiol* 2017; **46**: 234-241 [PMID: 28089690 DOI: 10.1067/j.cpradiol.2016.11.011]

11 **Qiu Y**, Zhang X, Wu Z, Wu S, Yang Z, Wang D, Le H, Mao J, Dai G, Tian X, Zhou R, Huang J, Hu L, Shen J. MRI-Based Radiomics Nomogram: Prediction of Axillary Non-Sentinel Lymph Node Metastasis in Patients With Sentinel Lymph Node-Positive Breast Cancer. *Front Oncol* 2022; **12**: 811347 [PMID: 35296027 DOI: 10.3389/fonc.2022.811347]

12 **Qu J**, Zhang H, Wang Z, Zhang F, Liu H, Ding Z, Li Y, Ma J, Zhang Z, Zhang S, Dong Y, Jiang L, Zhang W, Grimm R, Kiefer B, Kamel IR, Qin J, Li H. Comparison between free-breathing radial VIBE on 3-T MRI and endoscopic ultrasound for preoperative T staging of resectable oesophageal cancer, with histopathological correlation. *Eur Radiol* 2018; **28**: 780-787 [PMID: 28799124 DOI: 10.1007/s00330-017-4963-0]

13 **Giganti F**, Ambrosi A, Petrone MC, Canevari C, Chiari D, Salerno A, Arcidiacono PG, Nicoletti R, Albarello L, Mazza E, Gallivanone F, Gianolli L, Orsenigo E, Esposito A, Staudacher C, Del Maschio A, De Cobelli F. Prospective comparison of MR with diffusion-weighted imaging, endoscopic ultrasound, MDCT and positron emission tomography-CT in the pre-operative staging of oesophageal cancer: results from a pilot study. *Br J Radiol* 2016; **89**: 20160087 [PMID: 27767330 DOI: 10.1259/bjr.20160087]

14 **Lambin P**, Leijenaar RTH, Deist TM, Peerlings J, de Jong EEC, van Timmeren J, Sanduleanu S, Larue RTHM, Even AJG, Jochems A, van Wijk Y, Woodruff H, van Soest J, Lustberg T, Roelofs E, van Elmpt W, Dekker A, Mottaghy FM, Wildberger JE, Walsh S. Radiomics: the bridge between medical imaging and personalized medicine. *Nat Rev Clin Oncol* 2017; **14**: 749-762 [PMID: 28975929 DOI: 10.1038/nrclinonc.2017.141]

15 **Gillies RJ**, Kinahan PE, Hricak H. Radiomics: Images Are More than Pictures, They Are Data. *Radiology* 2016; **278**: 563-577 [PMID: 26579733 DOI: 10.1148/radiol.2015151169]

16 **Wang Y**, Zhu L, Xia W, Wang F. Anatomy of lymphatic drainage of the esophagus and lymph node metastasis of thoracic esophageal cancer. *Cancer Manag Res* 2018; **10**: 6295-6303 [PMID: 30568491 DOI: 10.2147/CMAR.S182436]

17 **Mönig S**, Chevallay M, Niclauss N, Zilli T, Fang W, Bansal A, Hoeppner J. Early esophageal cancer: the significance of surgery, endoscopy, and chemoradiation. *Ann N Y Acad Sci* 2018; **1434**: 115-123 [PMID: 30138532 DOI: 10.1111/nyas.13955]

18 **Nishimori H**, Hayashi S, Naito M, Murakami G, Fujita M, Hosokawa M. Mucosal lymphatic vessels of the esophagus distant from the cancer margin: morphometrical analysis using 27 surgically removed specimens of squamous cell carcinoma located in the upper or middle thoracic esophagus. *Okajimas Folia Anat Jpn* 2011; **88**: 43-47 [PMID: 22184865 DOI: 10.2535/ofaj.88.43]

19 **Markar S**, Gronnier C, Duhamel A, Pasquer A, Théreaux J, du Rieu MC, Lefevre JH, Turner K, Luc G, Mariette C. Salvage Surgery After Chemoradiotherapy in the Management of Esophageal Cancer: Is It a Viable Therapeutic Option? *J Clin Oncol* 2015; **33**: 3866-3873 [PMID: 26195702 DOI: 10.1200/JCO.2014.59.9092]

20 **Merkow RP**, Bilimoria KY, Keswani RN, Chung J, Sherman KL, Knab LM, Posner MC, Bentrem DJ. Treatment trends, risk of lymph node metastasis, and outcomes for localized esophageal cancer. *J Natl Cancer Inst* 2014; **106** [PMID: 25031273 DOI: 10.1093/jnci/dju133]

21 **Tong DK**, Law S, Kwong DL, Chan KW, Lam AK, Wong KH. Histological regression of squamous esophageal carcinoma assessed by percentage of residual viable cells after neoadjuvant chemoradiation is an important prognostic factor. *Ann Surg Oncol* 2010; **17**: 2184-2192 [PMID: 20217248 DOI: 10.1245/s10434-010-0995-2]

22 **Kim MP**, Correa AM, Lee J, Rice DC, Roth JA, Mehran RJ, Walsh GL, Ajani JA, Maru DM, Chang JY, Marom EM, Macapinlac HA, Lee JH, Vaporciyan AA, Rice T, Swisher SG, Hofstetter WL. Pathologic T0N1 esophageal cancer after neoadjuvant therapy and surgery: an orphan status. *Ann Thorac Surg* 2010; **90**: 884-90; discussion 890 [PMID: 20732513 DOI: 10.1016/j.athoracsur.2010.03.116]

23 **Sisic L**, Blank S, Weichert W, Jäger D, Springfeld C, Hochreiter M, Büchler M, Ott K. Prognostic impact of lymph node involvement and the extent of lymphadenectomy (LAD) in adenocarcinoma of the esophagogastric junction (AEG). *Langenbecks Arch Surg* 2013; **398**: 973-981 [PMID: 23887283 DOI: 10.1007/s00423-013-1101-6]

24 **Wang Q**, Yu S, Xiao Z, Liu X, Zhang W, Zhang X, He J, Sun K, Xu T, Feng Q, Zhou Z, Wang L, Yin W. Residual lymph node status is an independent prognostic factor in esophageal squamous cell Carcinoma with pathologic T0 after preoperative radiotherapy. *Radiat Oncol* 2015; **10**: 142 [PMID: 26159510 DOI: 10.1186/s13014-015-0450-4]

25 **Hölscher AH**, Bollschweiler E, Schröder W, Metzger R, Gutschow C, Drebber U. Prognostic impact of upper, middle, and lower third mucosal or submucosal infiltration in early esophageal cancer. *Ann Surg* 2011; **254**: 802-7; discussion 807 [PMID: 22042472 DOI: 10.1097/SLA.0b013e3182369128]

26 **van der Sluis PC**, Ruurda JP, Verhage RJ, van der Horst S, Haverkamp L, Siersema PD, Borel Rinkes IH, Ten Kate FJ, van Hillegersberg R. Oncologic Long-Term Results of Robot-Assisted Minimally Invasive Thoraco-Laparoscopic Esophagectomy with Two-Field Lymphadenectomy for Esophageal Cancer. *Ann Surg Oncol* 2015; **22** Suppl 3: S1350-S1356 [PMID: 26023036 DOI: 10.1245/s10434-015-4544-x]

27 **Omloo JM**, Lagarde SM, Hulscher JB, Reitsma JB, Fockens P, van Dekken H, Ten Kate FJ, Obertop H, Tilanus HW, van Lanschot JJ. Extended transthoracic resection compared with limited transhiatal resection for adenocarcinoma of the mid/distal esophagus: five-year survival of a randomized clinical trial. *Ann Surg* 2007; **246**: 992-1000; discussion 1000 [PMID: 18043101 DOI: 10.1097/sla.0b013e31815c4037]

28 **Hulscher JB**, van Sandick JW, de Boer AG, Wijnhoven BP, Tijssen JG, Fockens P, Stalmeier PF, ten Kate FJ, van Dekken H, Obertop H, Tilanus HW, van Lanschot JJ. Extended transthoracic resection compared with limited transhiatal resection for adenocarcinoma of the esophagus. *N Engl J Med* 2002; **347**: 1662-1669 [PMID: 12444180 DOI: 10.1056/nejmoa022343]

29 **Lordick F**, Mariette C, Haustermans K, Obermannová R, Arnold D; ESMO Guidelines Committee. Oesophageal cancer: ESMO Clinical Practice Guidelines for diagnosis, treatment and follow-up. *Ann Oncol* 2016; **27**: v50-v57 [PMID: 27664261 DOI: 10.1093/annonc/mdw329]

30 **DeMeester SR**. Adenocarcinoma of the esophagus and cardia: a review of the disease and its treatment. *Ann Surg Oncol* 2006; **13**: 12-30 [PMID: 16378161 DOI: 10.1245/aso.2005.12.025]

31 **Kelly S**, Harris KM, Berry E, Hutton J, Roderick P, Cullingworth J, Gathercole L, Smith MA. A systematic review of the staging performance of endoscopic ultrasound in gastro-oesophageal carcinoma. *Gut* 2001; **49**: 534-539 [PMID: 11559651 DOI: 10.1136/gut.49.4.534]

32 **Bruzzi JF**, Munden RF, Truong MT, Marom EM, Sabloff BS, Gladish GW, Iyer RB, Pan TS, Macapinlac HA, Erasmus JJ. PET/CT of esophageal cancer: its role in clinical management. *Radiographics* 2007; **27**: 1635-1652 [PMID: 18025508 DOI: 10.1148/rg.276065742]

33 **Schröder W**, Baldus SE, Mönig SP, Beckurts TK, Dienes HP, Hölscher AH. Lymph node staging of esophageal squamous cell carcinoma in patients with and without neoadjuvant radiochemotherapy: histomorphologic analysis. *World J Surg* 2002; **26**: 584-587 [PMID: 12098049 DOI: 10.1007/s00268-001-0271-5]

34 **Alper F**, Turkyilmaz A, Kurtcan S, Aydin Y, Onbas O, Acemoglu H, Eroglu A. Effectiveness of the STIR turbo spin-echo sequence MR imaging in evaluation of lymphadenopathy in esophageal cancer. *Eur J Radiol* 2011; **80**: 625-628 [PMID: 20800403 DOI: 10.1016/j.ejrad.2010.08.003]

35 **Sgourakis G**, Gockel I, Lyros O, Hansen T, Mildenberger P, Lang H. Detection of lymph node metastases in esophageal cancer. *Expert Rev Anticancer Ther* 2011; **11**: 601-612 [PMID: 21504265 DOI: 10.1586/era.10.150]

36 **Liu J**, Wang Z, Shao H, Qu D, Liu J, Yao L. Improving CT detection sensitivity for nodal metastases in oesophageal cancer with combination of smaller size and lymph node axial ratio. *Eur Radiol* 2018; **28**: 188-195 [PMID: 28677059 DOI: 10.1007/s00330-017-4935-4]

37 **Xu XQ**, Hu H, Su GY, Liu H, Hong XN, Shi HB, Wu FY. Utility of histogram analysis of ADC maps for differentiating orbital tumors. *Diagn Interv Radiol* 2016; **22**: 161-167 [PMID: 26829400 DOI: 10.5152/dir.2015.15202]

38 **Giganti F**, Salerno A, Ambrosi A, Chiari D, Orsenigo E, Esposito A, Albarello L, Mazza E, Staudacher C, Del Maschio A, De Cobelli F. Prognostic utility of diffusion-weighted MRI in oesophageal cancer: is apparent diffusion coefficient a potential marker of tumour aggressiveness? *Radiol Med* 2016; **121**: 173-180 [PMID: 26392393 DOI: 10.1007/s11547-015-0585-2]

39 **Shuto K**, Kono T, Shiratori T, Akutsu Y, Uesato M, Mori M, Narushima K, Imanishi S, Nabeya Y, Yanagawa N, Okazumi S, Koda K, Matsubara H. Diagnostic performance of diffusion-weighted magnetic resonance imaging in assessing lymph node metastasis of esophageal cancer compared with PET. *Esophagus* 2020; **17**: 239-249 [PMID: 31820208 DOI: 10.1007/s10388-019-00704-w]

40 **Sakurada A**, Takahara T, Kwee TC, Yamashita T, Nasu S, Horie T, Van Cauteren M, Imai Y. Diagnostic performance of diffusion-weighted magnetic resonance imaging in esophageal cancer. *Eur Radiol* 2009; **19**: 1461-1469 [PMID: 19172278 DOI: 10.1007/s00330-008-1291-4]

41 **Chen YL**, Li R, Chen TW, Ou J, Zhang XM, Chen F, Wu L, Jiang Y, Laws M, Shah K, Joseph B, Hu J. Whole-tumour histogram analysis of pharmacokinetic parameters from dynamic contrast-enhanced MRI in resectable oesophageal squamous cell carcinoma can predict T-stage and regional lymph node metastasis. *Eur J Radiol* 2019; **112**: 112-120 [PMID: 30777199 DOI: 10.1016/j.ejrad.2019.01.012]

42 **Sun NN**, Ge XL, Liu XS, Xu LL. Histogram analysis of DCE-MRI for chemoradiotherapy response evaluation in locally advanced esophageal squamous cell carcinoma. *Radiol Med* 2020; **125**: 165-176 [PMID: 31605354 DOI: 10.1007/s11547-019-01081-1]

43 **Azevedo RM**, de Campos RO, Ramalho M, Herédia V, Dale BM, Semelka RC. Free-breathing 3D T1-weighted gradient-echo sequence with radial data sampling in abdominal MRI: preliminary observations. *AJR Am J Roentgenol* 2011; **197**: 650-657 [PMID: 21862807 DOI: 10.2214/AJR.10.5881]

44 **Qu J**, Shen C, Qin J, Wang Z, Liu Z, Guo J, Zhang H, Gao P, Bei T, Wang Y, Liu H, Kamel IR, Tian J, Li H. The MR radiomic signature can predict preoperative lymph node metastasis in patients with esophageal cancer. *Eur Radiol* 2019; **29**: 906-914 [PMID: 30039220 DOI: 10.1007/s00330-018-5583-z]

45 **Tatsumi Y**, Tanigawa N, Nishimura H, Nomura E, Mabuchi H, Matsuki M, Narabayashi I. Preoperative diagnosis of lymph node metastases in gastric cancer by magnetic resonance imaging with ferumoxtran-10. *Gastric Cancer* 2006; **9**: 120-128 [PMID: 16767368 DOI: 10.1007/s10120-006-0365-8]

46 **Gatenby RA**, Grove O, Gillies RJ. Quantitative imaging in cancer evolution and ecology. *Radiology* 2013; **269**: 8-15 [PMID: 24062559 DOI: 10.1148/radiol.13122697]

47 **Zwanenburg A**, Vallières M, Abdalah MA, Aerts HJWL, Andrearczyk V, Apte A, Ashrafinia S, Bakas S, Beukinga RJ, Boellaard R, Bogowicz M, Boldrini L, Buvat I, Cook GJR, Davatzikos C, Depeursinge A, Desseroit MC, Dinapoli N, Dinh CV, Echegaray S, El Naqa I, Fedorov AY, Gatta R, Gillies RJ, Goh V, Götz M, Guckenberger M, Ha SM, Hatt M, Isensee F, Lambin P, Leger S, Leijenaar RTH, Lenkowicz J, Lippert F, Losnegård A, Maier-Hein KH, Morin O, Müller H, Napel S, Nioche C, Orlhac F, Pati S, Pfaehler EAG, Rahmim A, Rao AUK, Scherer J, Siddique MM, Sijtsema NM, Socarras Fernandez J, Spezi E, Steenbakkers RJHM, Tanadini-Lang S, Thorwarth D, Troost EGC, Upadhaya T, Valentini V, van Dijk LV, van Griethuysen J, van Velden FHP, Whybra P, Richter C, Löck S. The Image Biomarker Standardization Initiative: Standardized Quantitative Radiomics for High-Throughput Image-based Phenotyping. *Radiology* 2020; **295**: 328-338 [PMID: 32154773 DOI: 10.1148/radiol.2020191145]

48 **Li Y**, Beck M, Päßler T, Lili C, Hua W, Mai HD, Amthauer H, Biebl M, Thuss-Patience PC, Berger J, Stromberger C, Tinhofer I, Kruppa J, Budach V, Hofheinz F, Lin Q, Zschaeck S. A FDG-PET radiomics signature detects esophageal squamous cell carcinoma patients who do not benefit from chemoradiation. *Sci Rep* 2020; **10**: 17671 [PMID: 33077841 DOI: 10.1038/s41598-020-74701-w]

49 **Qiu Q**, Duan J, Deng H, Han Z, Gu J, Yue NJ, Yin Y. Development and Validation of a Radiomics Nomogram Model for Predicting Postoperative Recurrence in Patients With Esophageal Squamous Cell Cancer Who Achieved pCR After Neoadjuvant Chemoradiotherapy Followed by Surgery. *Front Oncol* 2020; **10**: 1398 [PMID: 32850451 DOI: 10.3389/fonc.2020.01398]

50 **Gu L**, Liu Y, Guo X, Tian Y, Ye H, Zhou S, Gao F. Computed tomography-based radiomic analysis for prediction of treatment response to salvage chemoradiotherapy for locoregional lymph node recurrence after curative esophagectomy. *J Appl Clin Med Phys* 2021; **22**: 71-79 [PMID: 34614265 DOI: 10.1002/acm2.13434]

51 **Tan X**, Ma Z, Yan L, Ye W, Liu Z, Liang C. Radiomics nomogram outperforms size criteria in discriminating lymph node metastasis in resectable esophageal squamous cell carcinoma. *Eur Radiol* 2019; **29**: 392-400 [PMID: 29922924 DOI: 10.1007/s00330-018-5581-1]

52 **Kim JY**, Seo HB, Park S, Moon JI, Lee JW, Lee NK, Lee SW, Bae YT. Early-stage invasive ductal carcinoma: Association of tumor apparent diffusion coefficient values with axillary lymph node metastasis. *Eur J Radiol* 2015; **84**: 2137-2143 [PMID: 26318821 DOI: 10.1016/j.ejrad.2015.08.009]

53 **Liu C**, Ding J, Spuhler K, Gao Y, Serrano Sosa M, Moriarty M, Hussain S, He X, Liang C, Huang C. Preoperative prediction of sentinel lymph node metastasis in breast cancer by radiomic signatures from dynamic contrast-enhanced MRI. *J Magn Reson Imaging* 2019; **49**: 131-140 [PMID: 30171822 DOI: 10.1002/jmri.26224]

54 **Shin J**, Seo N, Baek SE, Son NH, Lim JS, Kim NK, Koom WS, Kim S. MRI Radiomics Model Predicts Pathologic Complete Response of Rectal Cancer Following Chemoradiotherapy. *Radiology* 2022; **303**: 351-358 [PMID: 35133200 DOI: 10.1148/radiol.211986]

55 **Wang Q**, Xiang L, Liu J. Re: Feng G, Hong Y, Li L, *et al*. Anterior decompression and nonstructural bone grafting and posterior fixation for cervical facet dislocation with traumatic disc herniation. Spine (Phila Pa 1976). 2012;37:2082–8. *Spine (Phila Pa 1976)* 2013; **38**: 967 [PMID: 23660805 DOI: 10.1097/BRS.0b013e31828fc937]

56 **Santucci D**, Faiella E, Cordelli E, Sicilia R, de Felice C, Zobel BB, Iannello G, Soda P. 3T MRI-Radiomic Approach to Predict for Lymph Node Status in Breast Cancer Patients. *Cancers (Basel)* 2021; **13** [PMID: 34066451 DOI: 10.3390/cancers13092228]

57 **Han L**, Zhu Y, Liu Z, Yu T, He C, Jiang W, Kan Y, Dong D, Tian J, Luo Y. Radiomic nomogram for prediction of axillary lymph node metastasis in breast cancer. *Eur Radiol* 2019; **29**: 3820-3829 [PMID: 30701328 DOI: 10.1007/s00330-018-5981-2]

58 **Dong Y**, Feng Q, Yang W, Lu Z, Deng C, Zhang L, Lian Z, Liu J, Luo X, Pei S, Mo X, Huang W, Liang C, Zhang B, Zhang S. Preoperative prediction of sentinel lymph node metastasis in breast cancer based on radiomics of T2-weighted fat-suppression and diffusion-weighted MRI. *Eur Radiol* 2018; **28**: 582-591 [PMID: 28828635 DOI: 10.1007/s00330-017-5005-7]

59 **Liu J**, Sun D, Chen L, Fang Z, Song W, Guo D, Ni T, Liu C, Feng L, Xia Y, Zhang X, Li C. Radiomics Analysis of Dynamic Contrast-Enhanced Magnetic Resonance Imaging for the Prediction of Sentinel Lymph Node Metastasis in Breast Cancer. *Front Oncol* 2019; **9**: 980 [PMID: 31632912 DOI: 10.3389/fonc.2019.00980]

60 **Li M**, Zhang J, Dan Y, Yao Y, Dai W, Cai G, Yang G, Tong T. A clinical-radiomics nomogram for the preoperative prediction of lymph node metastasis in colorectal cancer. *J Transl Med* 2020; **18**: 46 [PMID: 32000813 DOI: 10.1186/s12967-020-02215-0]

World Journal of Radiology

Submit a Manuscript: https://www.f6publishing.com

World J Radiol 2023 July 28; 15(7): 226-233

DOI: 10.4329/wjr.v15.i7.226

ISSN 1949-8470 (online)

ORIGINAL ARTICLE

Basic Study

Can the change of vasomotor activity in irritable bowel syndrome patients be detected *via* color Doppler ultrasound?

Omer Kazci, Fahrettin Ege, Huseyin Aydemir, Saliha Kazci, Sonay Aydin

Specialty type: Radiology, nuclear medicine and medical imaging

Provenance and peer review: Invited article; Externally peer reviewed.

Peer-review model: Single blind

Peer-review report's scientific quality classification

Grade A (Excellent): 0
Grade B (Very good): B
Grade C (Good): C
Grade D (Fair): 0
Grade E (Poor): 0

P-Reviewer: Baeg MK, South Korea; Lv L, China

Received: April 25, 2023
Peer-review started: April 25, 2023
First decision: June 19, 2023
Revised: June 20, 2023
Accepted: July 7, 2023
Article in press: July 7, 2023
Published online: July 28, 2023

Omer Kazci, Department of Radiology, Ankara Training and Research Hospital, Ankara 06600, Turkey

Fahrettin Ege, Department of Neurology, VM Medicalpark Hospital, Ankara 06600, Turkey

Huseyin Aydemir, Sonay Aydin, Department of Radiology, Erzincan Binali Yildirim University Mengucek Gazi Training and Research Hospital, Erzincan 24400, Turkey

Saliha Kazci, Department of Epidemiology, Ankara University Faculty of Medicine, Ankara 06600, Turkey

Corresponding author: Sonay Aydin, MD, PhD, Academic Editor, Associate Professor, Department of Radiology, Erzincan Binali Yildirim University Mengucek Gazi Training and Research Hospital, Başbağlar, Hacı Ali Akın Cd. No. 32, 24100 Erzincan Merkez/Erzincan, Erzincan 24400, Turkey. sonay.aydin@erzincan.edu.tr

Abstract

BACKGROUND

Irritable bowel syndrome (IBS) is one of the most frequently referred conditions to the gastrointestinal outpatient clinic. The pathophysiology of IBS has not been determined with certainty. Visceral hypersensitivity is indicated as one of the pathophysiologies. The sympathetic nervous system is primarily in charge of controlling the arteries, and its effect is vasospasm in the medium and large arteries, resulting in decreased blood flow.

AIM

To demonstrate, using Doppler evaluation of the brachial artery, that sympathetic activity impairs vasomotor performance due to autonomic neuropathy, which we believe is associated with IBS.

METHODS

There were 58 participants in the study. The control group consisted of 29 healthy patients, while the remaining 29 patients had been diagnosed with IBS. Patients who met the Rome IV criteria and had IBS were included in the study. People with known polyneuropathy or non-IBS chronic conditions that can progress were excluded from the trial, as were those with essential hypertension, diabetes mellitus, cardiovascular disease, or peripheral arterial disease, and patients diagnosed with anxiety or depression. Those with moderate to severe carpal

tunnel syndrome or a median nerve lesion due to trauma were also excluded from the trial. A Doppler probe was used to measure the baseline diameter and flow rates of the brachial artery from 2 cm superior to the antecubital fossa. The Doppler probe remained stationary throughout the experiment, allowing for continuous measurements. Then, to activate the sympathetic fibers, an electrical stimulus for 5 s with an intensity of 10 mA and a frequency of 1 Hz was applied to the median nerve at the wrist level *via* the bipolar stimulus electrode. The artery diameter and flow rates were measured again immediately following the fifth stimulus.

RESULTS

In healthy persons with no history of chronic illness, there was a statistically significant decrease in flow rate after stimulation ($P < 0.001$). In addition, stimulation resulted in a statistically significant reduction in the diameter of the brachial artery ($P < 0.001$). Patients diagnosed with IBS had statistically significant vasodilation and an increase in flow rate.

CONCLUSION

Sympathetic stimulation causes a reduction in vascular diameter and blood flow, whereas it has the reverse effect on IBS patients. In investigating the involvement of autonomic neuropathy in the development of IBS, significant changes in brachial artery Doppler parameters were observed before and after stimulation of the median nerve with low-current sensory stimulation. This method is thought to be more user-friendly and comfortable than other methods described in the literature.

Key Words: Irritable bowel syndrome; Doppler ultrasonography; Brachial artery; Median nerve; Peripheral neuropathy; Autonomic neuropathy

Core Tip: It has been noted that the autonomic activity of individuals who suffer from irritable bowel syndrome (IBS) differs from that of healthy people. Colored Doppler ultrasonography can be utilized as a noninvasive diagnostic tool that can be performed at any age and at any age, is comfortable for the patient, and does not require further patient compliance to show autonomic dysfunction in patients with IBS.

Citation: Kazci O, Ege F, Aydemir H, Kazci S, Aydin S. Can the change of vasomotor activity in irritable bowel syndrome patients be detected *via* color Doppler ultrasound? *World J Radiol* 2023; 15(7): 226-233
URL: https://www.wjgnet.com/1949-8470/full/v15/i7/226.htm
DOI: https://dx.doi.org/10.4329/wjr.v15.i7.226

INTRODUCTION

Irritable bowel syndrome (IBS) is a common chronic disease that causes constipation, diarrhea, or both, as well as abdominal pain or cramps, and can significantly reduce quality of life and work productivity. The diagnosis can be made with confidence if organic diseases are ruled out and characteristic symptoms are present. Environmental factors such as stress, food intolerance, enteric infections, and antibiotics, as well as patient-related factors such as variability in pain perception, variability in brain-gut interaction, dysbiosis, increased intestinal permeability, increased intestinal mucosal immune activation, and visceral hypersensitivity, are considered potential etiologies[1,2]. The autonomic nervous system modulates visceral sensitivity, and the central nervous system influences gastrointestinal secretion and activity *via* the enteric nervous system and autonomic pathways[3,4].

Some studies have found differences in autonomic activity between IBS subgroups. In studies with IBS and control groups, in patients with IBS, in the study of Karling *et al*[5], the heart rate variability was evaluated in the supine position with the head 70° upwards; an increase in sympathetic nervous system activation was observed, but no significant change in parasympathetic nervous system activation was found[5]. Adeyemi *et al*[6] investigated heart rate variability under orthostatic stress, deep inspiration, and resting states and discovered an increase in sympathetic nervous system activation and a decrease in parasympathetic nervous system activation[6]. Van Orshoven *et al*[7] measured blood pressure, heart rate, heart rate variability, and muscle sympathetic nerve activity before, during, and after a standard meal. As a result, parasympathetic nervous system activation decreased while sympathetic nervous system activation increased. There was no discernible difference[7]. Tanaka *et al*[8] investigated fingertip blood flow during, before, and after cold stress and discovered an increase in sympathetic nervous system activation[8]. Spaziani *et al*[9] used baroreceptor sensitivity to assess heart rate and blood pressure variability before, during, and after rectal distension and found a decrease in baroreceptor sensitivity and an increase in blood pressure[9]. In a study by Yildirim *et al*[10], neuropathy tests (standing, Valsalva, deep inspiration, isometric exercise, and cold application) were evaluated, and it was discovered that sympathetic activity increased while parasympathetic activity decreased[10].

Doppler ultrasonography is a type of ultrasonographic imaging that is used to determine the morphology of vascular structures as well as the direction, amount, and shape of blood flow in them. The laser Doppler method is widely used to assess sympathetic vasoconstrictor function. In the literature, it is emphasized that continuous wave Doppler ultrasound is a valid alternative approach to laser Doppler flowmetry in healthy volunteers[11], as well as that it can be used to detect the normal and abnormal functioning of the peripheral sympathetic nervous system[12]. The benefits of using color Doppler ultrasonography include the fact that it has no known side effects, does not contain radiation, can be used at any time and age including pregnancy, is easy to apply, does not require additional patient compliance, and is a noninvasive diagnostic method.

Almost all research into autonomic dysfunction in IBS is out of date. The goal of this study was to determine if autonomic dysfunction can be demonstrated in IBS patients using this new color Doppler ultrasonography (CDUS)-based method, as well as to reevaluate the presence of autonomic dysfunction in IBS, which has been described in previous studies.

MATERIALS AND METHODS

The participants signed a declaration form declaring that all participants and/or their legal guardians granted informed permission. The studies adhered to the most recent edition of the Declaration of Helsinki, and the Ankara City Hospital No. 2 Clinical Research Ethics Committee authorized the procedures.

Patients who met the Rome IV criteria and had IBS were included in the study. People with known polyneuropathy or non-IBS chronic conditions that can progress were excluded from the trial, as were those with essential hypertension, diabetes mellitus, cardiovascular disease, peripheral arterial disease, and patients diagnosed with anxiety or depression. Those with moderate to severe carpal tunnel syndrome or a median nerve lesion due to trauma were also excluded from the trial.

The technical models are associated with "studies on sensory nerve conduction." These non-invasive approaches are utilized in routine clinical electrophysiological examinations to detect peripheral neuropathies. Four hours before the experiment, nicotine, caffeine, alcohol, and exercise were restricted. Before measuring the subjects' blood pressure, heart rate, and body temperature, they rested for 10 min in a seated position with their forearms supinated. The study was carried out at temperatures between 22 C and 24 C. Individuals were encouraged to remain as motionless as possible and were verbally informed at each test stage following a 10-min rest period (for example, before the Doppler measurement was performed and before the electrical stimulation began). The diameter and flow rates of the right brachial artery were measured from 2 cm above the antecubital fossa using a 9 Hz linear probe of the LOQIC P9 USG Doppler device (GE Healthcare, Chicago, IL, United States) (Figure 1A). A radiologist with 8 years of experience in Doppler took these readings. The Doppler sensor remained stationary during the experiment, allowing for continuous readings. Then an electrical stimulation of 10 mA intensity and 1 Hz frequency was applied to the median nerve at the level of the wrist for 5 s using the bipolar stimulus electrode of the Neuropack S1 MEB-9400A EMG/EP system (Nihon Kohden Co., Tokyo, Japan), in the direction of the sensory fibers (orthodromically) (Figure 1B). Immediately after the sixth stimulation, artery diameter and flow rates were measured again. Some demonstrative examinations can be seen in Figures 2 and 3.

In addition to sociodemographic data such as age and sex, the diameters and flow rates of the brachial arteries were recorded as final data before and after electrical stimulation in the healthy control group and IBS patients.

Statistical analyses

The variables were investigated using analytical methods (Kolmogorov-Smirnov/Shapiro-Wilk's test) to determine whether they were normally distributed. Descriptive analyses were presented using frequencies and percentages for the categorical variables, mean ± SD for normally distributed variables, and median (25P-75P) for the non-normally distributed variables. The Student's *t*-test or Mann–Whitney U test was used for the comparison of continuous variables in independent groups, and the paired samples *t*-test was used in dependent groups. $P < 0.05$ was considered statistically significant. Statistical analyses were performed using SPSS (20.0; Armonk, NY, United States).

RESULTS

The study included 58 people, 29 of whom were diagnosed with IBS and 29 of whom were in the control group. Thirty (51.7%) of the 58 participants in the study were women, with a median age of 36 (min-max: 18-64). The female/male ratios (51.7%/48.3%) were the same in both groups ($P = 1.000$), and the median age of the IBS group [36 (min-max: 31-48)] was comparable to that of the control group [36 (min-max: 30-49)] ($P = 0.864$).

Table 1 shows brachial artery flow measurements before and after median nerve stimulation in IBS and control groups. While the median pre-stimulation flow rate in the IBS group was 60.2 mL/min, the post-stimulation flow rate was 78.1 mL/min. Mean flow rates before and after stimulation in the control group were 77.5 and 39.7 mL/min, respectively. The decrease in flow seen in the control group with median nerve stimulation could not be replicated in the IBS group.

Before median nerve stimulation, the mean brachial artery diameter in the IBS group was 3.44 mm, while it was 3.43 mm in the control group. While the diameters measured before median stimulation in the IBS and control groups were not statistically different ($P = 0.092$), the diameters measured after stimulation were statistically significant ($P < 0.001$). While median nerve stimulation caused a decrease in diameter in the control group, it caused an increase in the IBS group

Table 1 Brachial artery flow measurements before and after stimulation according to ırritable bowel syndrome and control groups

	Pre-stimulation flow rate (mL/min), mean ± SD	Post-stimulation flow rate (mL/min), mean ± SD	*P* value
IBS (n = 29)	60.2 ± 28.8	78.1 ± 42.5	0.002
Control (n = 29)	77.5 ± 36.5	39.7 ± 19.1	< 0.001
P value	0.05	< 0.001	

IBS: Irritable bowel syndrome.

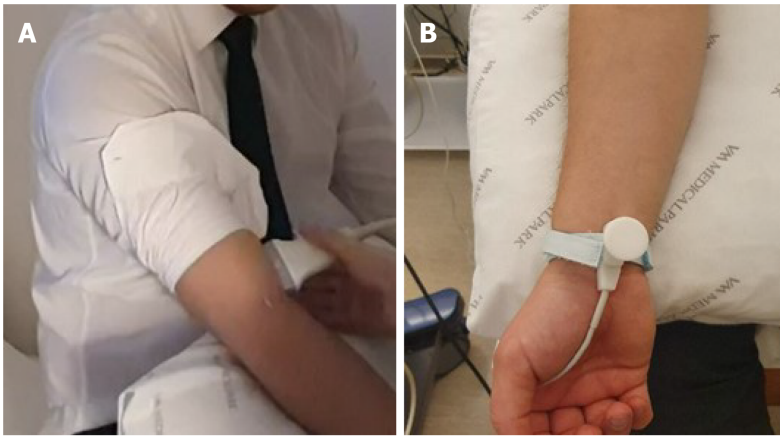

DOI: 10.4329/wjr.v15.i7.226 **Copyright** ©The Author(s) 2023.

Figure 1 Positioning of the Doppler ultrasound probe and bipolar stimulus electrode. A: Positioning of the Doppler ultrasound probe, 2 cm above the antecubital fossa using a 9 Hz linear probe; B: Positioning of the bipolar stimulus electrode.

(Table 2).

Before the stimulus, there was no significant difference in the flow rate and artery diameters between the control and study groups (Tables 1 and 2).

Table 3 shows the changes in brachial artery flow and diameter measurements after median nerve stimulation. While there was a median increase in brachial artery output of 9.10 (min-max: 0.00-33.70) mL/min and a median increase in brachial artery diameter of 0.20 (min-max: 0.00-0.40) mm in the IBS group, the changes in flow and diameter were decreased in the control group. Median brachial artery output was 33.00 (min-max: 24.20-42.50) mL/min, and median brachial artery diameter was 0.50 (min-max: 0.40-0.90) mm in the control group. The participants in the IBS and control groups had a significant difference in brachial artery flow rates (P < 0.001) and diameters (P < 0.001) before and after median nerve stimulation. The change in flow and diameter after stimulation was statistically significant in both the IBS and control groups (P < 0.001 for both sexes).

By evaluating the changes in brachial artery flow (Table 4) and diameter (Table 5) according to the presence of chronic disease in the male and female groups, statistical significance was maintained for both sexes. In other words, the change in flow and diameter following stimulation was statistically significant (P < 0.001 for both sexes) in both the IBS and control groups.

DISCUSSION

The primary goal of our research was to use CDUS to detect autonomic dysfunction in IBS patients. In our study, there was an increase in brachial artery diameter and flow rate in IBS patients measured with Doppler ultrasonography before and after median nerve stimulation, whereas there was a decrease in the control group.

Changes in flow and diameter after median nerve stimulation were found to be statistically significant in both IBS patients and the control group, regardless of sex. This is the first study to compare autonomic dysfunction in IBS patients based on age and sex, and to use CDUS to assess sympathetic autonomic functions in IBS patients.

Previously, Eicke *et al*[11] used continuous-wave Doppler ultrasound and laser Doppler flowmetry to detect blood flow changes in the radial artery during sympathetic stimulation (deep breathing and coughing) and compared the two methods. They discovered a decrease in flow in the radial artery after sympathetic stimulation using both continuous-wave Doppler ultrasound and laser Doppler flowmetry. As a result, they determined that continuous-wave Doppler ultrasound can be used in blood flow measurements after sympathetic stimulation as laser Doppler flowmetry[11].

Several studies have reported differences in sympathetic and parasympathetic autonomic activity in IBS patients. The majority of these studies looked at both sympathetic and parasympathetic activity.

Table 2 Brachial artery diameter measurements before and after stimulation according to IBS and control groups

	Diameter before stimulus (mm), mean ± SD	Diameter after stimulus (mm), mean ± SD	*P* value
IBS	3.4 ± 0.5	3.7 ± 0.5	0.01
Control	3.4 ± 0.5	2.8 ± 0.6	< 0.001
P value	0.92	< 0.001	

IBS: Irritable bowel syndrome.

Table 3 Changes in brachial artery flow and diameter with stimulation

	Flow difference before and after stimulus (mL/min), median (25P-75P)	Diameter difference before and after stimulus (mm), median (25P-75P)
IBS	9.10 (0.00-33.70)	0.20 (0.00-0.40)
Control	-33.00 (-42.50 to -24.20)	-0.50 (-0.90 to -0.40)
P value	< 0.001	< 0.001

IBS: Irritable bowel syndrome; P: Percentile.

Table 4 The difference in flow rate between ırritable bowel syndrome and the control group before and after stimulation, according to gender

		The difference in flow rate between before and after a stimülation (mL/min), median (25P-75P)	*P* value
Female	IBS (*n* = 15)	11.90 (0.00-35.70)	< 0.001
	Control (*n* = 15)	-25.50 (-39.40 to -21.60)	
Male	IBS (*n* = 14)	6.55 (-0.60-25.50)	< 0.001
	Control (*n* = 14)	-39.75 (-58.90 to -32.00)	

IBS: Irritable bowel syndrome; P: Percentile.

Table 5 Diameter difference before and after stimulation between ırritable bowel syndrome and control groups according to sex

		The difference in diameter between before and after a stimulation (mm), median (25P-75P)	*P* value
Female	IBS (*n* = 15)	0.20 (0.00-0.40)	< 0.001
	Control (*n* = 15)	-0.50 (-1.00 to -0.30)	
Male	IBS (*n* = 14)	0.30 (0.00-0.50)	< 0.001
	Control (*n* = 14)	-0.60 (-0.90 to -0.40)	

IBS: Irritable bowel syndrome; P: Percentile.

Karling *et al*[5] investigated autonomic activity differences in their study, which included 18 patients with IBS and 36 control groups, by evaluating heart rate variability in the supine position with the head 70° upwards. When compared to healthy people, IBS patients showed an increase in sympathetic nervous system activation but no significant change in parasympathetic nervous system activation[5].

Adeyemi *et al*[6] investigated autonomic activity differences in 35 patients with IBS and 18 control groups in a study that included orthostatic stress, deep inspiration, and resting-state heart rate variability. In the study, IBS patients had an increase in sympathetic nervous system activation at rest and a decrease in parasympathetic nervous system activation under orthostatic stress and deep inspiration compared to healthy individuals[6].

Van Orshoven *et al*[7] investigated autonomic activity differences and muscle sympathetic nerve activity in 18 patients with IBS and 19 control groups by evaluating blood pressure, heart rate, and heart rate variability during, before, and

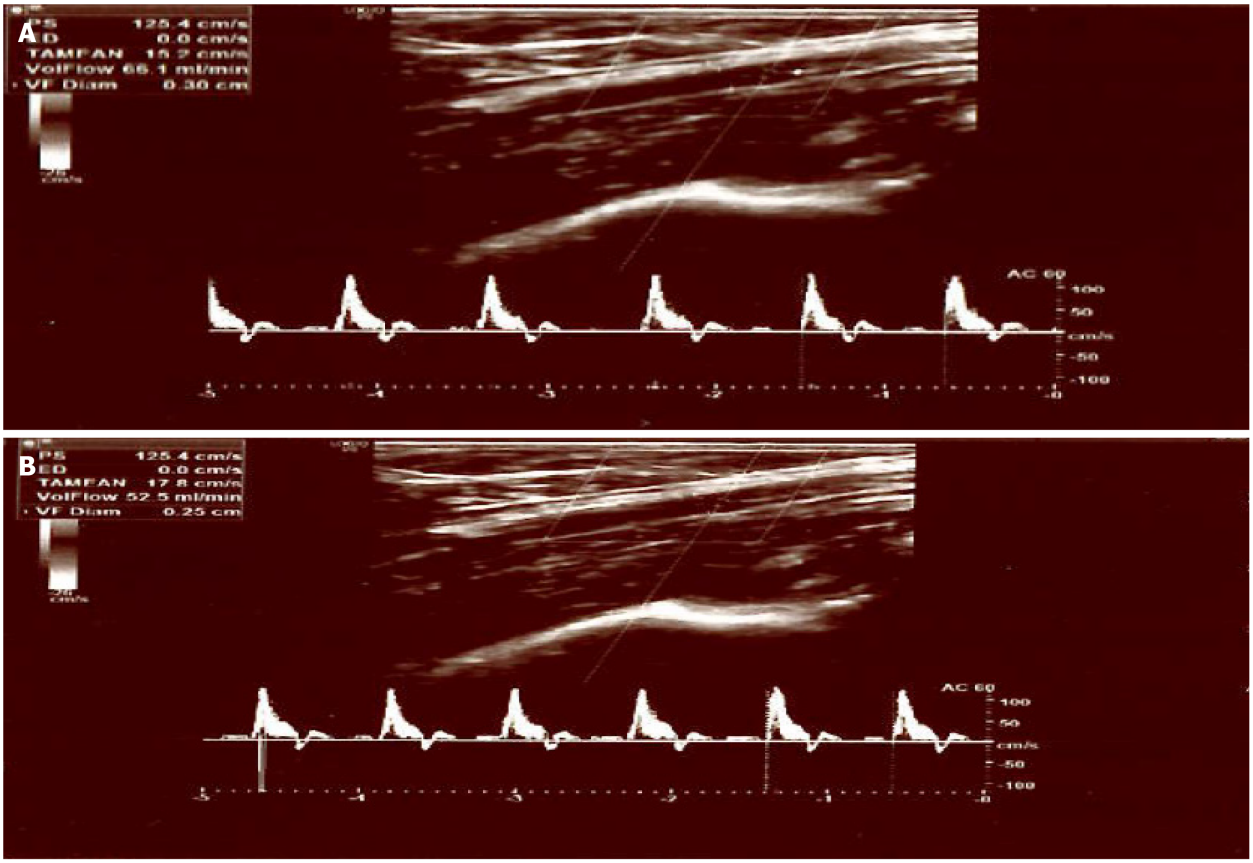

DOI: 10.4329/wjr.v15.i7.226

Figure 2 Before and after electrical stimulation, the brachial artery flow/diameter parameters at control participant. A: Before electrical stimulation, the brachial artery volume flow rates/diameter values of a 45-year-old healthy control participant were measured to be 66.1 mL/min, 3 mm; B: The post-stimulation values of the same patient were 52.5 mL/min, 2.5 mm.

after consumption of a standard meal. When IBS patients were compared to healthy people, there was no decrease in parasympathetic nervous system activation, an increase in sympathetic nervous system activation, or a significant change in muscle sympathetic nerve activity[7].

The study group and control group were monitored, and autonomic neuropathy tests (standing posture, Valsalva, deep inspiration, isometric exercise, and cold application) were used in the study conducted by Yildirim *et al*[10], which included 50 patients with IBS and 49 control groups. The study discovered that when IBS patients were compared to healthy people, sympathetic activity increased while parasympathetic activity decreased[10].

There are also studies that only assessed sympathetic system dysfunction.

Tanaka *et al*[8] investigated autonomic activity differences in 59 patients with IBS and 40 control groups by measuring fingertip blood flow during, before, and after cold stress. In the study, IBS patients had higher levels of sympathetic nervous system activation than healthy people[8].

Spaziani *et al*[9] used baroreceptor sensitivity to assess heart rate and blood pressure variability before, during, and after rectal distension in 39 patients with IBS and 98 control groups. In the study, IBS patients were found to have lower baroreceptor sensitivity and a higher increase in blood pressure after rectal distension when compared to healthy individuals[9].

We have demonstrated, as in previous studies, that autonomic dysfunction exists in IBS patients. The method we used in our study is low-cost, simple, and comfortable for the patient, and it does not necessitate additional patient compliance. We described a novel method for demonstrating sympathetic autonomic dysfunction in IBS patients.

Our research had some limitations. The fact that CDUS measurements of brachial artery diameter and flow are user-dependent adds to the measurement's subjectivity. A single researcher measured everything in a single session. As a result, interobserver and intraobserver variability cannot be shown. Furthermore, the study's limitations include the relatively small study population and the fact that IBS subtypes were not evaluated separately. Another limitation of the current study was the lack of investigation into parasympathetic autonomic functions.

CONCLUSION

Our findings show that a new CDUS-based method can successfully detect sympathetic autonomic dysfunction in IBS patients. This method is thought to be more user-friendly and comfortable than other methods described in the literature.

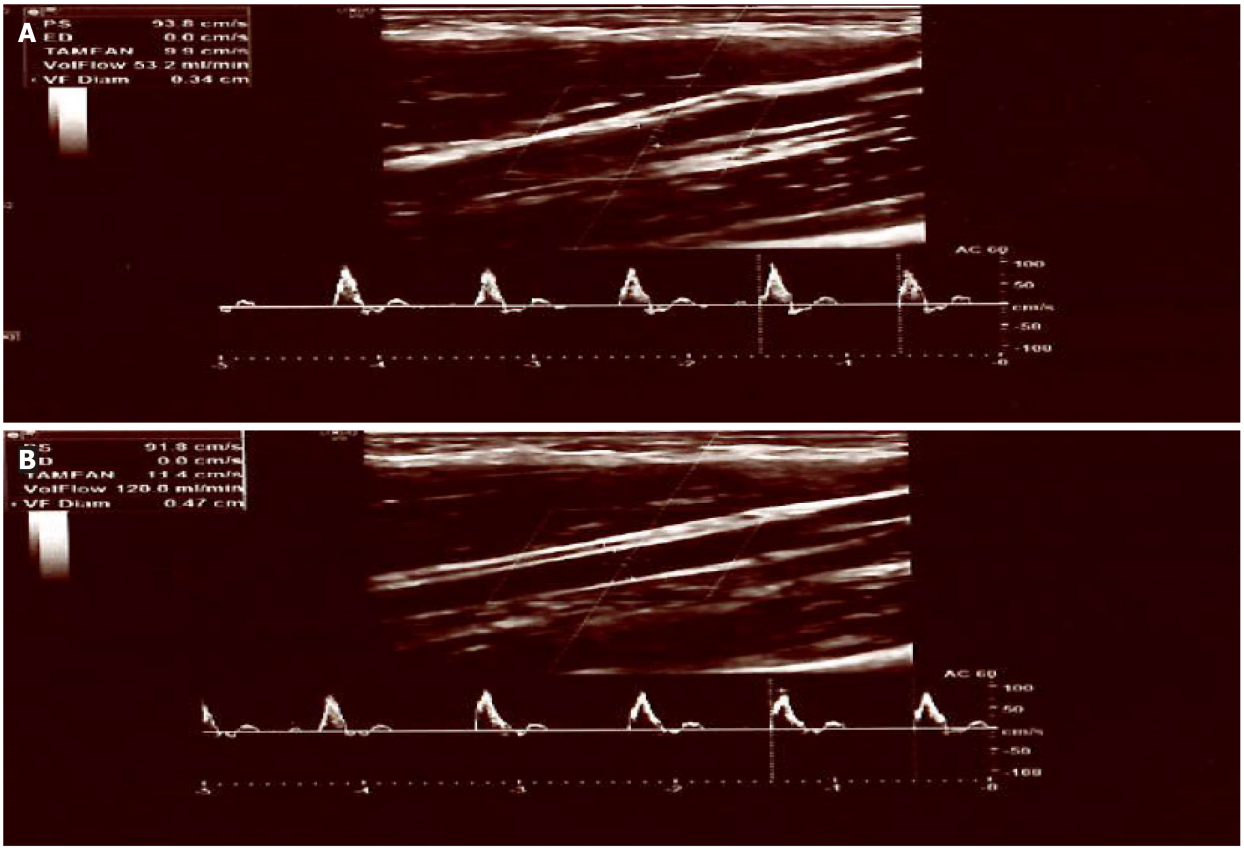

DOI: 10.4329/wjr.v15.i7.226

Figure 3 Before and after electrical stimulation, the brachial artery flow/diameter parameters in a patient diagnosed with irritable bowel syndrome. A: Before electrical stimulation, the brachial artery flow/diameter parameters of a 38-year-old female patient diagnosed with irritable bowel syndrome were assessed to be 53.2 mL/min, 3.2 mm; B: The post-stimulation values of the same patient were 120 mL/min, 4.7 mm.

ARTICLE HIGHLIGHTS

Research background

Irritable bowel syndrome (IBS) is one of the most common illnesses referred to the gastrointestinal outpatient clinic. The pathophysiology of IBS is not completely understood. One of the pathophysiologies is visceral hypersensitivity. The sympathetic nervous system is primarily responsible for managing the arteries, and its consequence is vasospasm in the medium and large arteries, which results in decreased blood flow.

Research motivation

Our impetus came from our study's adoption of a novel approach to assess changes in vasomotor activity in IBS patients.

Research objectives

We wanted to employ a different way to determine the change in vasomotor activity in persons with IBS in our study.

Research methods

The diameter and flow velocities of the brachial artery were determined using a probe with Doppler examination at the diameter of the antecubital fossa. To activate the sympathetic fibers, bipolar stimulation was applied to the median nerve at the wrist. Brachial artery diameter and flow velocities were assessed again immediately after the fifth stimulation.

Research results

In our study, a statistically significant decrease was found in brachial artery flow velocity and diameter after sympathetic stimulation in healthy individuals without a history of chronic disease. In patients with IBS, a statistically significant increase was found in brachial artery flow velocity and diameter after sympathetic stimulation.

Research conclusions

As a result, sympathetic activation reduces artery width and blood flow in healthy people. In people with IBS, it has the opposite effect. Detection of changes in brachial artery diameter and flow velocity by Doppler examination is thought to be more useful and comfortable than other methods described in the literature.

Research perspectives

It has been discovered that the autonomic activity of persons suffering from IBS differs from that of healthy people. Colored Doppler ultrasonography can be used as a noninvasive diagnostic method that can be conducted at any age, is comfortable for the patient, and does not require additional patient compliance in patients with IBS.

FOOTNOTES

Author contributions: Kazci O, Ege F, and Kazci S contributed equally to this work; Aydemir H wrote the manuscript; Aydin S, Kazci S, and Kazci O performed the experiments; Aydemir H and Ege F provided technical support and suggestions; Aydin S participated in writing and modifying the manuscript; Kazci O designed the study; All authors approved the final manuscript.

Institutional review board statement: The studies adhered to the most recent edition of the Declaration of Helsinki, and the Ankara City Hospital No. 2 Clinical Research Ethics Committee authorized the procedures, No. E2-22-1307.

Informed consent statement: The participants signed a declaration form declaring that all participants and/or their legal guardians granted informed permission.

Conflict-of-interest statement: All the authors report no relevant conflicts of interest for this article.

Data sharing statement: No additional data are available.

Country/Territory of origin: Turkey

ORCID number: Omer Kazci 0000-0003-0846-1074; Fahrettin Ege 0000-0001-9502-7510; Huseyin Aydemir 0000-0002-5698-1560; Saliha Kazci 0000-0002-8937-9939; Sonay Aydin 0000-0002-3812-6333.

S-Editor: Li L
L-Editor: Filipodia
P-Editor: Zhao S

REFERENCES

1 **Chey WD**, Kurlander J, Eswaran S. Irritable bowel syndrome: a clinical review. *JAMA* 2015; **313**: 949-958 [PMID: 25734736 DOI: 10.1001/jama.2015.0954]
2 **Camilleri M**. Diagnosis and Treatment of Irritable Bowel Syndrome: A Review. *JAMA* 2021; **325**: 865-877 [PMID: 33651094 DOI: 10.1001/jama.2020.22532]
3 **Iovino P**, Azpiroz F, Domingo E, Malagelada JR. The sympathetic nervous system modulates perception and reflex responses to gut distention in humans. *Gastroenterology* 1995; **108**: 680-686 [PMID: 7875470 DOI: 10.1016/0016-5085(95)90439-5]
4 **Gibbons CH**. Basics of autonomic nervous system function. *Handb Clin Neurol* 2019; **160**: 407-418 [PMID: 31277865 DOI: 10.1016/B978-0-444-64032-1.00027-8]
5 **Karling P**, Nyhlin H, Wiklund U, Sjöberg M, Olofsson BO, Bjerle P. Spectral analysis of heart rate variability in patients with irritable bowel syndrome. *Scand J Gastroenterol* 1998; **33**: 572-576 [PMID: 9669625 DOI: 10.1080/00365529850171800]
6 **Adeyemi EO**, Desai KD, Towsey M, Ghista D. Characterization of autonomic dysfunction in patients with irritable bowel syndrome by means of heart rate variability studies. *Am J Gastroenterol* 1999; **94**: 816-823 [PMID: 10086672 DOI: 10.1111/j.1572-0241.1999.00861.x]
7 **van Orshoven NP**, Andriesse GI, van Schelven LJ, Smout AJ, Akkermans LM, Oey PL. Subtle involvement of the parasympathetic nervous system in patients with irritable bowel syndrome. *Clin Auton Res* 2006; **16**: 33-39 [PMID: 16477493 DOI: 10.1007/s10286-006-0307-x]
8 **Tanaka T**, Manabe N, Hata J, Kusunoki H, Ishii M, Sato M, Kamada T, Shiotani A, Haruma K. Characterization of autonomic dysfunction in patients with irritable bowel syndrome using fingertip blood flow. *Neurogastroenterol Motil* 2008; **20**: 498-504 [PMID: 18248583 DOI: 10.1111/j.1365-2982.2007.01039.x]
9 **Spaziani R**, Bayati A, Redmond K, Bajaj H, Mazzadi S, Bienenstock J, Collins SM, Kamath MV. Vagal dysfunction in irritable bowel syndrome assessed by rectal distension and baroreceptor sensitivity. *Neurogastroenterol Motil* 2008; **20**: 336-342 [PMID: 18179607 DOI: 10.1111/j.1365-2982.2007.01042.x]
10 **Yildirim AE**, Korkmaz M, Altun R, Sandikçi SC, Ocal S, Selçuk H. Is there any association between irritable bowel syndrome subgroups and autonomous dysfunction. *Eur Rev Med Pharmacol Sci* 2016; **20**: 1315-1322 [PMID: 27097952]
11 **Eicke BM**, Milke K, Schlereth T, Birklein F. Comparison of continuous wave Doppler ultrasound of the radial artery and laser Doppler flowmetry of the fingertips with sympathetic stimulation. *J Neurol* 2004; **251**: 958-962 [PMID: 15316800 DOI: 10.1007/s00415-004-0471-7]
12 **Kazci O**, Ege F. Evaluation of Sympathetic Vasomotor Activity of the Brachial Arteries Using Doppler Ultrasound. *Med Sci Monit* 2023; **29**: e939352 [PMID: 36908037 DOI: 10.12659/MSM.939352]

World Journal of Radiology

Submit a Manuscript: https://www.f6publishing.com

World J Radiol 2023 July 28; 15(7): 234-240

DOI: 10.4329/wjr.v15.i7.234

ISSN 1949-8470 (online)

CASE REPORT

Invasive rhinocerebral mucormycosis: Imaging the temporal evolution of disease in post COVID-19 case with diabetes: A case report

Ramakrishna Narra, Shravya Rayapati

Specialty type: Radiology, nuclear medicine and medical imaging

Provenance and peer review: Unsolicited article; Externally peer reviewed.

Peer-review model: Single blind

Peer-review report's scientific quality classification

Grade A (Excellent): 0
Grade B (Very good): 0
Grade C (Good): C, C
Grade D (Fair): 0
Grade E (Poor): 0

P-Reviewer: Jain M, India; Yu YB, China

Received: April 3, 2023
Peer-review started: April 3, 2023
First decision: May 19, 2023
Revised: June 2, 2023
Accepted: June 26, 2023
Article in press: June 26, 2023
Published online: July 28, 2023

Ramakrishna Narra, Shravya Rayapati, Department of Radiodiagnosis, Katuri Medical College, Guntur, Andhra Pradesh 522018, India

Corresponding author: Ramakrishna Narra, DNB, MD, MNAMS, Academic Editor, Professor, Department of Radiodiagnosis, Katuri Medical College, Flat No. 30, 1/2 Chandramoulinagar, Guntur, Andhra Pradesh 522018, India. narra.ramki29@gmail.com

Abstract

BACKGROUND

Rhinocerebral mucormycosis (RCM) is a rare, fatal, invasive fungal infection infecting mainly patients with immunocompromised conditions, such as diabetes mellitus, hematologic malignancies, and organ transplantations. Coronavirus disease 2019 (COVID-19) disease in these patients further weakens the immune system due to several factors, including hypoxia, corticosteroid usage (further increasing hyperglycemic status), mechanical ventilation, increased serum ferritin levels, endothelitis due to free radicals, and glucose receptor protein upregulation. Timely diagnosis, judicious treatment decisions, and diabetes control with proper treatment guidelines in patients with coexisting COVID-19 disease can reduce complication rates and improve survival.

CASE SUMMARY

A 75-year-old male patient with diabetes and hypertension diagnosed with COVID-19 presented to the emergency department. Laboratory examinations revealed elevated blood glucose levels, as well as ketone bodies in the urine. He was treated with oxygen and steroids, as well as insulin to correct blood glucose levels. He complained of a headache 10 d later, and imaging demonstrated mucosal thickening in bilateral sphenoidal, ethmoidal, and maxillary sinuses with hyperdense foci in the right maxillary sinus but without central nervous system involvement. Surgical debridement was performed, and a histopathological study revealed fungi hyphae. Systemic antifungals (amphotericin b and posaconazole) were administered. Subsequently, on 15th day he developed right lower limb weakness and left lateral rectus palsy. There was slow but steady progress, and he was discharged. However, he presented to emergency department 1mo later with altered sensorium and poor control of diabetes resulted in an intracranial spread of mucormycosis, which ultimately led to the patient's poor prognosis and slow recovery.

CONCLUSION
Prompt early diagnosis, judicious treatment decisions, and diabetes control with proper treatment guidelines are necessary in patients with COVID-19 associated invasive RCM to reduce complication rates and improve patient survival.

Key Words: Rhinocerebral mucormycosis; COVID-19 disease; Corticosteroids; Diabetes mellitus; Diabetic ketoacidosis; Case report

Core Tip: Coronavirus disease 2019 associated invasive rhinocerebral mucormycosis is potentially life threatening in patients with uncontrolled diabetes mellitus and diabetic ketoacidosis. Early diagnosis and imaging the disease progression with proper treatment guidelines are essential for reducing the morbidity and mortality in these patients.

Citation: Narra R, Rayapati S. Invasive rhinocerebral mucormycosis: Imaging the temporal evolution of disease in post COVID-19 case with diabetes: A case report. *World J Radiol* 2023; 15(7): 234-240
URL: https://www.wjgnet.com/1949-8470/full/v15/i7/234.htm
DOI: https://dx.doi.org/10.4329/wjr.v15.i7.234

INTRODUCTION

Mucormycosis is a rare opportunistic and potentially lethal infection caused by members of the family mucoraceae, order mucorales, and class zygomycetes[1]. It is caused by fungi, which may be found in decaying food, soil, or other organic matter, such as animal excreta.

Rhinocerebral mucormycosis (RCM) is the most common type, accounting for 30%-50% of cases. Its extension to the orbit and brain is usual, making it a potentially life-threatening disease. Immunocompromised patients are especially susceptible, and timely diagnosis and judicious intervention are of utmost importance for the successful management and prevention of intracranial extension. Patients with coronavirus disease 2019 (COVID-19) with uncontrolled diabetes and diabetic ketoacidosis on corticosteroid treatment are potentially susceptible to invasive RCM and need aggressive treatment to prevent further morbidity and mortality. Other reported immunocompromised conditions include blood dyscrasias, malnutrition, neutropenia, iron overload, organ transplantation, and immunosuppressive therapy[2]. Microscopic demonstration of fungal hyphae-mucormycosis with high blood glucose levels and serum ferritin and ketone levels should alert the clinician for appropriate care and aggressive treatment[3].

CASE PRESENTATION

Chief complaints

A 75-year-old male patient diagnosed with positive reverse transcription polymerase chain reaction for COVID-19 infection was admitted to the emergency department.

History of present illness

A 75-year-old male patient diagnosed with positive reverse transcription polymerase chain reaction for COVID-19 infection was admitted to the emergency department with fever, sore throat and generalized weakness for 3 d.

On 10th day he complained of frontal headache. On 15th day he complained of persistent frontal headache and left orbital pain, and a dragging sensation in the right foot. After 1 mo he progressed into altered sensorium and seizures and was admitted to emergency department.

History of past illness

He is known diabetic and hypertensive for 10 years.

Personal and family history

No significant personal and family history.

Physical examination

On examination at admission temperature was 102.5 ^{0}F, pulse rate: 124/min, blood pressure (BP): 150/100 mmHg.

On 10th day temperature was 101.5 ^{0}F, pulse rate: 88/min, BP: 150/90 mmHg. On 15th day temperature was 99 ^{0}F, pulse rate: 108/min, BP: 130/90 mmHg, neurological examination revealed reduced power in the right lower limb (2/5) and

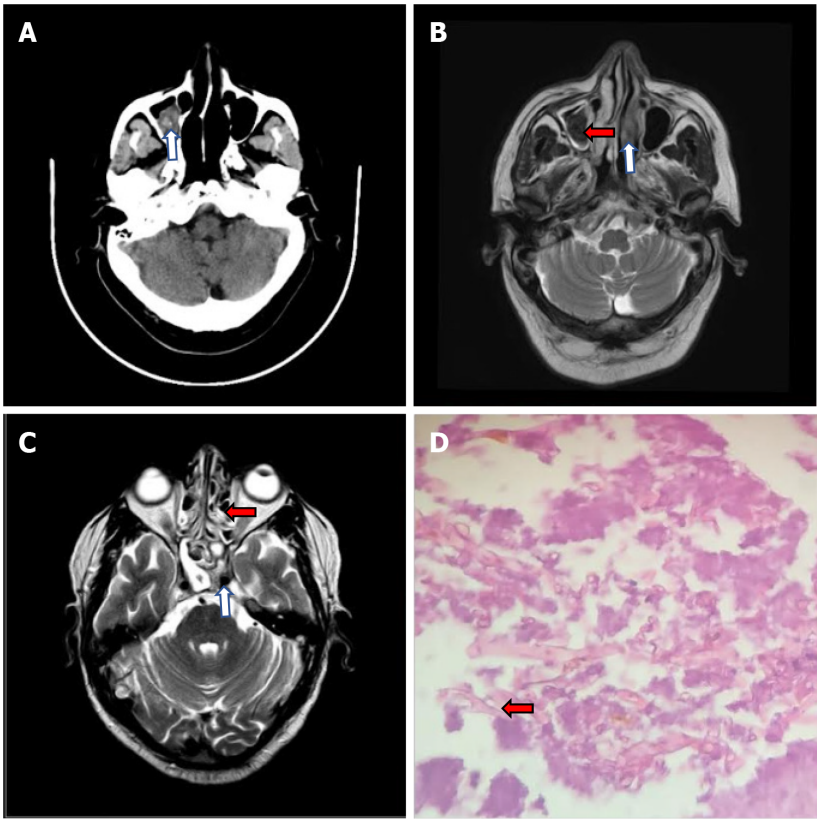

DOI: 10.4329/wjr.v15.i7.234 **Copyright** ©The Author(s) 2023.

Figure 1 Images of patient with post COVID-19 mucormycosis. A: Axial computed tomography image of brain, 10 d post admission demonstrating hyperdensity in right maxillary sinus (white arrow); B: Axial T2 weighted (T2W) and magnetic resonance imaging (MRI) image of brain demonstrating mucosal thickening with hypointensity within right maxillary sinus (red arrow) and hypointense left inferior turbinate (white arrow); C: Axial T2W and MRI image of brain demonstrating bilateral sphenoid and ethmoidal sinusitis (red arrow) with normal flow void within left internal carotid artery (white arrow); D: Histopathology slide demonstrating broad, aseptate ,branched hyphae of mucormycosis (red arrow).

left lateral rectus palsy. On 30th day temperature was 102 ^{0}F, pulse rate: 115/min, BP: 160/100 mmHg, glasgow coma scale was poor (8/15).

Laboratory examinations

On admission: Elevated C-reactive protein (188 mg/dL), serum ferritin (513 ng/mL), blood glucose (400 mg/dL), and glycosylated hemoglobin (16%) levels and the presence of ketone bodies (+++) in the urine. Other parameters were within the normal limits: Hemoglobin of 11 gm%; red blood cells of 5.2 × 10^{6}/μL; total leukocyte count of 9000/cumm; differential leukocyte count, including neutrophils of 75%, lymphocytes of 22%, eosinophils of 02%, and macrophages of 01%; platelets of 2.4 Lakhs/cumm; serum potassium of 3.8 mmol/L; serum sodium of 138 mmol/L; blood urea of 12 mg/dL; and serum creatinine of 0.8 mg/dL.

On 10th day C-reactive protein (106 mg/dL), serum ferritin (498 ng/mL), blood glucose (260 mg/dL), and the presence of ketone bodies (+) in the urine.

On 15th day C-reactive protein (108 mg/dL), serum ferritin (450 ng/mL), blood glucose (250 mg/dL), and the presence of ketone bodies (+) in the urine.

After 1 mo C-reactive protein (198 mg/dL), serum ferritin (415 ng/mL), blood glucose (450 mg/dL), and the presence of ketone bodies (+++) in the urine.

Rest of the routine laboratory investigations were within normal limits.

Imaging examinations

On 10th day post admission computed tomography (CT) and magnetic resonance imaging (MRI) demonstrated mucosal thickening in the bilateral ethmoidal, sphenoidal and maxillary sinuses with hyperdensity (CT) and hypointensity (MRI) in the right maxillary sinus suggestive of fungal sinusitis (Figure 1A-C). The patient underwent functional endoscopic sinus surgery under general anesthesia, and a biopsy was performed for histopathological examination which revealed fungus of mucorales species (Figure 1D).

On 15th day post admission MRI scan of the brain, paranasal sinuses and the orbits with IV contrast was advised which demonstrated acute infarcts in the watershed territories of left anterior cerebral artery, middle cerebral artery and posterior cerebral arteries (Figure 2A-D) with filling defects in the left cavernous sinus suggestive of cavernous sinus thrombosis. In addition magnetic resonance angiogram demonstrated complete occlusion of left internal carotid artery (ICA) (Figure 2E and F).

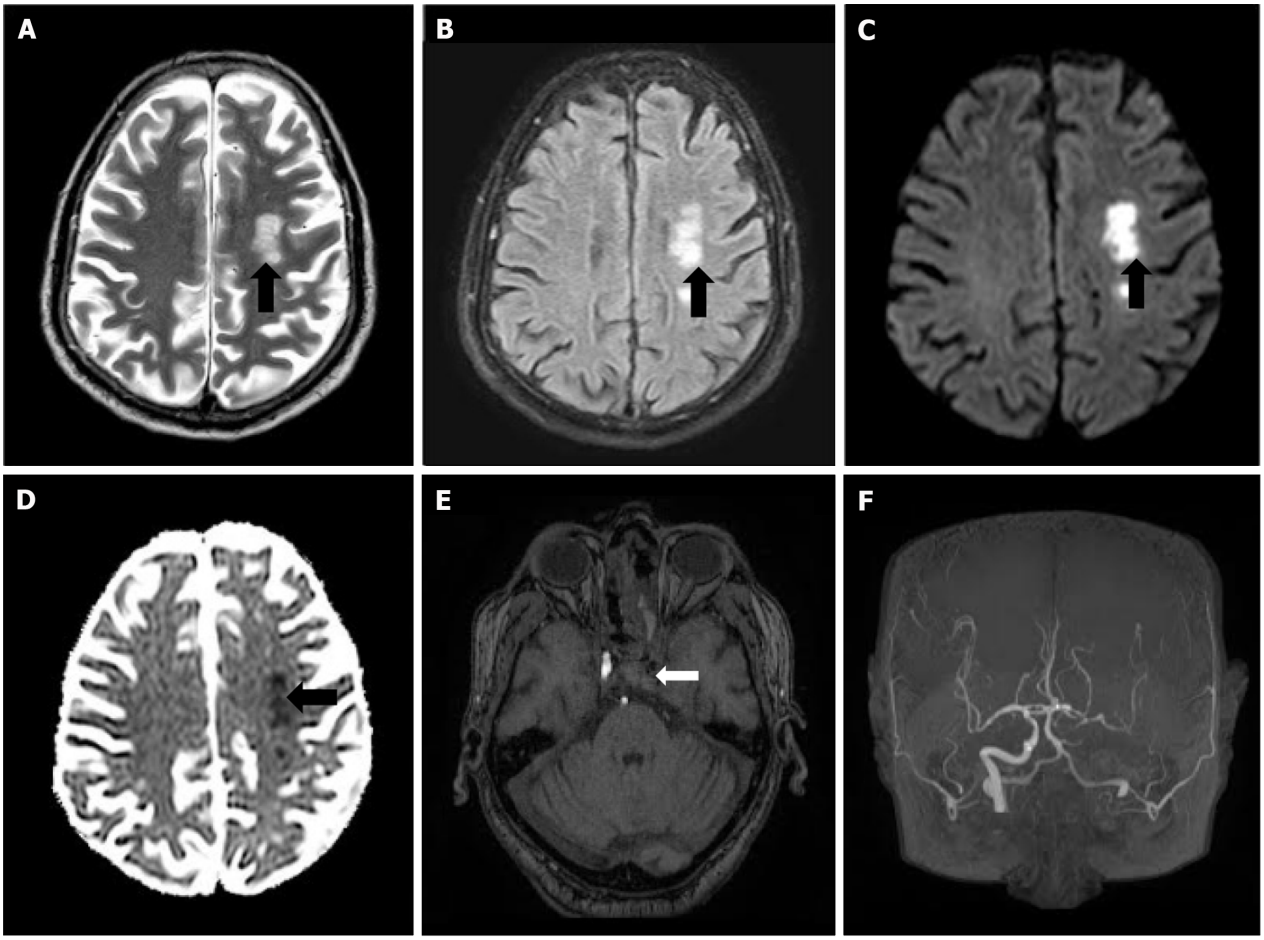

DOI: 10.4329/wjr.v15.i7.234 **Copyright** ©The Author(s) 2023.

Figure 2 Images of patient with post COVID-19 mucormycosis. A and B: Axial T2-weighted and axial fluid attenuated inversion recovery images of brain 15 d post admission demonstrating acute infarcts (black arrows); C and D: In left centrum semiovale with diffusion restriction on diffusion-weighted imaging and reversal on apparent diffusion coefficient represented by black arrows; E and F: Magnetic resonance angiography (MRA) images of Brain demonstrating loss of flow signal is noted in left internal carotid artery (white arrow) on source images and absent left internal carotid artery on maximum intensity projection MRA.

After 1 mo MRI of brain with IV contrast demonstrated an hyperintense lesion on T2 Weighted and fluid attenuated inversion recovery sequence with surrounding edema and peripheral rim enhancement of approximately 21 mm × 12 mm in the right basi-frontal lobe with restriction on diffusion weighted imaging and reduced apparent diffusion coefficient suggestive of fungal abscess (Figure 3). CT and MRI of brain demonstrated destruction of cribriform plate, clivus, sphenoid sinus and magnetic resonance spectroscopy demonstrated elevated lactate peak within the lesion (Figure 4).

FINAL DIAGNOSIS

Post COVID-19 associated invasive RCM.

TREATMENT

On admission: Patient was given mechanical ventilation and oxygen support, anti-pyretics, azithromycin, remedesivir (200 mg loading dose) followed by 100 mg daily for 5 d, and intravenous dexamethasone 10 mg intravenous for 10 d. The patient was administered insulin 0.1 U/kg as an intravenous bolus dose followed by infusion of 0.1 U/kg/h for a targeted glucose level of 200 mg/dL.

On 10th day: The patient was advised and started with amphotericin b injection at 3 mg/kg/day for 14 d and oral posaconazole at 300 mg twice daily for 6 wk. The renal profile was checked every 3 d for nephrotoxicity from amphotericin b. Poor patient tolerance was noted and steroids discontinued.

On 15th day: The patient was administered aspirin 150 mg, clopitab 75 mg, and atorvastatin 40 mg. After stabilization and rehabilitation patient was counselled for diabetes control and discharged. He was maintained on human mixtard insulin thrice daily.

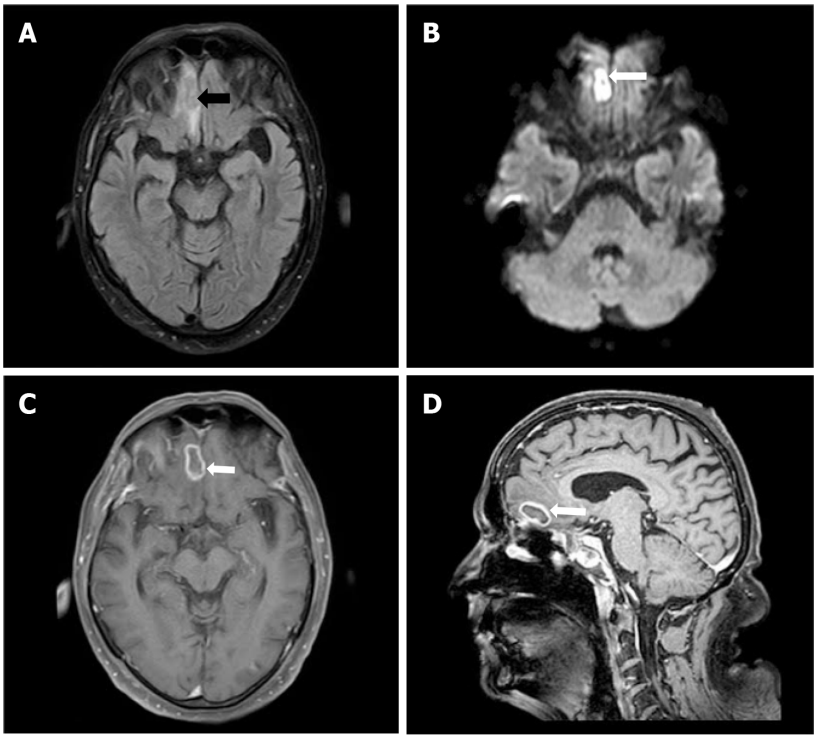

DOI: 10.4329/wjr.v15.i7.234 **Copyright** ©The Author(s) 2023.

Figure 3 Images of patient with post COVID-19 mucormycosis. A and B: Magnetic resonance imaging of brain after one month demonstrating isointense area with surrounding edema (black arrow) on axial fluid attenuated inversion recovery with restriction on diffusion-weighted imaging (white arrow); C and D: Post-contrast axial and sagittal T1 weighted images demonstrating rim enhancement of the lesion-s/ofungal abscess (white arrow).

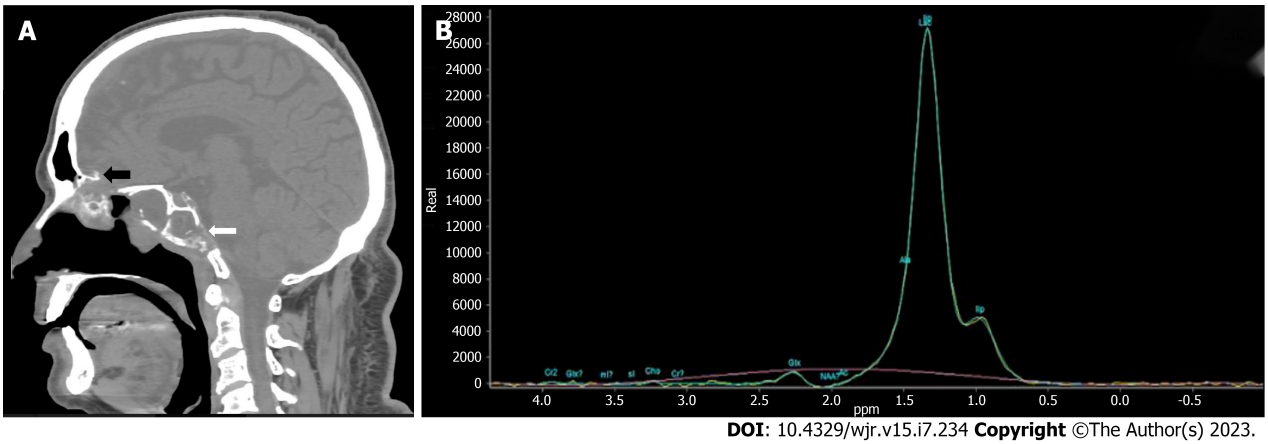

DOI: 10.4329/wjr.v15.i7.234 **Copyright** ©The Author(s) 2023.

Figure 4 Images of patient with post COVID-19 mucormycosis. A: Computerized tomography of brain after one month mid sagittal reformatted section in bone window demonstrating destruction of cribriform plate (black arrow), sphenoid sinus and clivus (white arrow); B: Magnetic resonance spectroscopy with a voxel placed in right frontal lobe fungal abscess demonstrating lactate peak at 1.33 ppm.

After 1mo: The patient was treated with antiepileptics, and insulin and anti-fungal treatment was continued with supportive treatment.

OUTCOME AND FOLLOW-UP

After stabilization there was very slow recovery of the patient with residual neurological deficits and increased morbidity.

DISCUSSION

RCM is a rare invasive infection caused by fungi of the class phycomycetes commonly involving the nasal and sinus mucosae of immunocompromised patients and spreads rapidly to the orbit and brain. Diabetes mellitus (especially with ketoacidosis) and hematologic malignancies with neutropenia are the principal predisposing factors. High blood glucose levels and ketoacidosis in diabetes enhance fungal growth. The altered number or function of neutrophils increases the risk of infection because they are responsible for defense against fungi[3]. COVID-19 disease in these patients further weakens the immune system due to several factors, including hypoxia, corticosteroid usage (further increasing hyperglycemic status), mechanical ventilation, increased serum ferritin levels, endothelitis due to free radicals, and glucose receptor protein upregulation, increased iron reduces the function of gamma interferon which prevents phagocytic function on fungus[4]. Other identified risk factors are steroid therapy, organ transplantation, chemotherapy, and chronic kidney disease[5-7]. Extensive angioinvasion is considered the main cause of vascular thrombosis and tissue necrosis. Vascular involvement is a more common cause of increased morbidity and mortality, resulting in ICA thrombosis causing brain ischemic infarcts and infiltrating the cavernous sinus and orbital apex, causing facial cellulitis and vision loss. Histopathological examination of the thrombus demonstrated the fungus in some cases of ICA thrombosis following thrombectomy[8]. Mucormycosis may spread intracranially from the paranasal sinuses along the cribriform plate into the anterior cranial fossa, leading to a cerebral abscess.

Brain and paranasal sinus MRI provides a better evaluation of intracranial and soft tissue involvement, skull base invasion, perineural spread, and vascular obstruction. MRI contrast study demonstrates orbital soft tissue invasion, skull base infiltration, perineural spread, intracranial complications, and vascular obstruction, involving the ICA[9,10].

At present, antifungal therapy and aggressive surgical debridement are used in active mucormycosis treatment. The overall mortality of patients with mucormycosis remains high and approaches 40% in patients with diabetes with invasive mucormycosis despite antifungal therapy and surgical debridement. Prophylactic treatment with antiplatelet drugs, including aspirin, clopitab, and statins, should also be initiated in aggressive cases where complications, such as ICA occlusion, thrombosis, and angioinvasion may develop.

Our case report explains the disease progression from infection initially involving the paranasal sinuses to subsequent brain involvement. Mucosal thickening of the bilateral sphenoidal, ethmoidal, and maxillary sinuses was initially noted on imaging in the present report, with no central nervous system involvement with a normal ICA and without any bony involvement. However, ICA thrombosis causing ischemic infarcts was noted on subsequent imaging, probably due to poor patient compliance to antifungal drugs causing increased fungal growth. The patient was stabilized and treated with aspirin 150 mg, clopitab 75 mg, and atorvastatin 40 mg and rehabilitation. However, the patient was readmitted to the hospital with seizures and altered consciousness after a few days, and subsequent imaging revealed the spread of infection through the destruction of the cribriform plate and clivus to the brain causing a cerebral abscess. This was due to poor diabetes control and diabetic ketoacidosis after patient discharge, which caused the intracranial spread of the disease.

CONCLUSION

Invasive RCM is a rare but fatal fungal infection that primarily affects immunocompromised patients. Early diagnosis and prompt management with aggressive surgical intervention and antifungal therapy are crucial for improving patient outcomes. This case report highlights the importance of close monitoring and imaging in patients with post-COVID-19 treated with oxygen therapy and corticosteroids, as well as diabetes, and ensuring optimal glycemic control to prevent rapid disease progression and intracranial spread. Regular monitoring of serum ferritin levels, lymphocyte count and further strengthening the immune system with regular follow-up imaging is essential to monitor disease progression and identify potential complications.

ACKNOWLEDGEMENTS

Dr Rama Krishna Gorantla for his expert advice and guidance.

FOOTNOTES

Author contributions: Narra R reviewed the manuscript and designed the study; Rayapati S prepared the manuscript, and collected materials for the study.

Informed consent statement: Informed written consent was obtained from the patient and his relatives for the publication of this report and any accompanying images.

Conflict-of-interest statement: All the authors report no relevant conflicts of interest for this article.

CARE Checklist (2016) statement: The authors have read the CARE Checklist (2016) and the manuscript was prepared and revised according to the CARE Checklist (2016).

Country/Territory of origin: Mayotte

ORCID number: Ramakrishna Narra 0000-0002-1850-6136.

S-Editor: Qu XL
L-Editor: A
P-Editor: Zhao S

REFERENCES

1 **Kim JG**, Park HJ, Park JH, Baek J, Kim HJ, Cha IH, Nam W. Importance of immediate surgical intervention and antifungal treatment for rhinocerebral mucormycosis: a case report. *J Korean Assoc Oral Maxillofac Surg* 2013; **39**: 246-250 [PMID: 24471053 DOI: 10.5125/jkaoms.2013.39.5.246]
2 **Mallis A**, Mastronikolis SN, Naxakis SS, Papadas AT. Rhinocerebral mucormycosis: an update. *Eur Rev Med Pharmacol Sci* 2010; **14**: 987-992 [PMID: 21284348]
3 **Dilek A**, Ozaras R, Ozkaya S, Sunbul M, Sen EI, Leblebicioglu H. COVID-19-associated mucormycosis: Case report and systematic review. *Travel Med Infect Dis* 2021; **44**: 102148 [PMID: 34454090 DOI: 10.1016/j.tmaid.2021.102148]
4 **Aggarwal SK**, Kaur U, Talda D, Pandey A, Jaiswal S, Kanakan A, Singh A, Chakrabarti SS. Case Report: Rhino-orbital Mucormycosis Related to COVID-19: A Case Series Exploring Risk Factors. *Am J Trop Med Hyg* 2021; **106**: 566-570 [PMID: 34902834 DOI: 10.4269/ajtmh.21-0777]
5 **Spellberg B**, Edwards J Jr, Ibrahim A. Novel perspectives on mucormycosis: pathophysiology, presentation, and management. *Clin Microbiol Rev* 2005; **18**: 556-569 [PMID: 16020690 DOI: 10.1128/CMR.18.3.556-569.2005]
6 **Bhansali A**, Bhadada S, Sharma A, Suresh V, Gupta A, Singh P, Chakarbarti A, Dash RJ. Presentation and outcome of rhino-orbital-cerebral mucormycosis in patients with diabetes. *Postgrad Med J* 2004; **80**: 670-674 [PMID: 15537854 DOI: 10.1136/pgmj.2003.016030]
7 **Onyango JF**, Kayima JK, Owen WO. Rhinocerebral mucormycosis: case report. *East Afr Med J* 2002; **79**: 390-393 [PMID: 12638836 DOI: 10.4314/eamj.v79i7.8845]
8 **Kashyap S**, Bernstein J, Ghanchi H, Bowen I, Cortez V. Diagnosis of Rhinocerebral Mucormycosis by Treatment of Cavernous Right Internal Carotid Artery Occlusion With Mechanical Thrombectomy: Special Case Presentation and Literature Review. *Front Neurol* 2019; **10**: 264 [PMID: 30972005 DOI: 10.3389/fneur.2019.00264]
9 **McDevitt GR Jr**, Brantley MJ, Cawthon MA. Rhinocerebral mucormycosis: a case report with magnetic resonance imaging findings. *Clin Imaging* 1989; **13**: 317-320 [PMID: 2598114 DOI: 10.1016/0899-7071(89)90065-x]
10 **Parsi K**, Itgampalli RK, Vittal R, Kumar A. Perineural spread of rhino-orbitocerebral mucormycosis caused by Apophysomyces elegans. *Ann Indian Acad Neurol* 2013; **16**: 414-417 [PMID: 24101833 DOI: 10.4103/0972-2327.116921]

Published by **Baishideng Publishing Group Inc**
7041 Koll Center Parkway, Suite 160, Pleasanton, CA 94566, USA
Telephone: +1-925-3991568
E-mail: bpgoffice@wjgnet.com
Help Desk: https://www.f6publishing.com/helpdesk
https://www.wjgnet.com